Error Rate Analysis of Amplitude-Coherent Detection over Rician Fading Channels with Receiver Diversity

Error Rate Analysis of Amplitude-Coherent Detection over Rician Fading Channels with Receiver Diversity

Mohammad Al-Jarrah[†], Ki-Hong Park[‡], Arafat Al-Dweik[†], and Mohamed-Slim Alouini[‡]
[†]Khalifa University of Science and Technology, Abu Dhabi, UAE.
E-mail: {mohammad.aljarrah, arafat.dweik}@ku.ac.ae.
[‡]King Abdullah University of Science and Technology (KAUST), Thuwal, Kingdom of Saudi Arabia.
E-mail: { kihong.park, slim.alouini}@kaust.edu.sa.

February 6, 2019

Abstract

Amplitude-coherent (AC) detection is an efficient detection technique that can simplify the receiver design while providing reliable symbol error rate (SER). Therefore, this work considers AC detector design and SER analysis using M-ary amplitude shift keying (MASK) modulation over Rician fading channels. More specifically, we derive the optimum, near-optimum and a suboptimum AC detectors and compare their SER to the coherent, noncoherent and the heuristic AC detectors. Moreover, the analytical SER of the heuristic detector is derived using two different approaches for single and multiple receiving antennas. One of the derived expressions is expressed in terms of a single integral that can be evaluated numerically, while the second approach gives a closed-form analytical expression for the SER, which is also used to derive a simple formula for the asymptotic SER at high signal-to-noise ratios (SNRs). The obtained analytical and simulation results show that the SER of the AC and coherent MASK detectors are comparable, particularly for high values of the Rician K-factor, and small number of receiving antennas. Moreover, the obtained results show that the SER of the optimal AC detector is equivalent to that of the coherent detector. However, the optimal AC detector complexity is prohibitively high, particularly at high SNRs. In most of the scenarios, the heuristic AC detector significantly outperforms the optimum noncoherent detector, except for the binary ASK case at low SNRs. Moreover, the obtained results show that the heuristic AC detector is immune to phase noise, and thus, it outperforms the coherent detector in scenarios where system is subject to considerable phase noise.

keywords: Optical wireless communications (OWC), free space optics (FSO), non-coherent, semi-coherent, amplitude-coherent, Rician, Ricean, receiver diversity, phase noise.

1 Introduction

Generally speaking, there are three main types of detection schemes for digital signals, which are coherent detection, noncoherent detection, and partially coherent detection [1]. The detector design, required channel state information (CSI), computational complexity, and symbol error rate (SER) of each detection scheme depend on several factors such as the modulation scheme, modulation order, and channel model. Therefore, adopting a particular modulation and detection schemes is mostly determined by the targeted application. For example, broadband communications require spectrally efficient modulation schemes to support high data rates, and the communicating nodes typically have sufficient resources to estimate the CSI, and hence, modulation schemes with high order and coherent detectors are utilized. For most wireless applications, quadrature amplitude modulation (QAM) is considered as the most attractive

due to its power and spectral efficiency [2]-[4]. Nevertheless, M-ary amplitude shift keying (MASK) has recently attracted extensive attention because it is more suitable for certain applications such as wireless sensor networks (WSNs) [5], wireless energy transfer [6], radio frequency identification (RFID) [7], and optical wireless communications (OWC) [8]-[12].

Unlike typical wireless communications systems, OWC such as free space optics (FSO) and visible light communications (VLC) that use intensity modulation with direct detection (IM-DD) require the baseband signal to be real and positive, and hence, using QAM for OWC directly is infeasible. To overcome this limitation, QAM can be combined with orthogonal frequency division multiplexing (OFDM) to generate real and positive signals using various techniques [13]. Nevertheless, the spectral efficiency and SER of QAM-OFDM is generally equivalent to MASK-OFDM [14]. Therefore, MASK renders itself as an efficient alternative to QAM for OWC [15] because it can be used with/without OFDM. Moreover, in IM-DD, the binary ASK (BASK) can be detected using a simple noncoherent detector that does not require prior knowledge of the instantaneous CSI. The noncoherent BASK detector has low complexity and robust to hardware impairments such as the carrier frequency offset and phase noise, but it suffers from poor spectral efficiency, and accurate knowledge of the statistical CSI is necessary to compute the optimum threshold. Improving the spectral efficiency of noncoherent MASK modulation by increasing the modulation order M is not feasible in fading channels due to its poor symbol error rate (SER) [1], which limits its utilization to additive white Gaussian noise (AWGN) channels. Practically speaking, the AWGN channel model is limited to few applications such as indoor OWC [13].

Although the channel in OWC may be considered non-fading in certain scenarios [16], [17], channel models that consider the fading induced by atmospheric turbulence can be considered more practical, and they are actually more flexible because they can be used to describe a wide range of fading scenarios. In the literature, several channel models have been adopted for OWC including the Gamma-Gamma, exponential and Rician [13], [18], [19]. Moreover, the random pointing error in OWC are typically modeled as Rician [20]-[22]. The Rician channel model is of particular interest because it is also widely adopted in wireless communications systems, such as massive multiple-input multiple-output (MIMO) systems [23]-[27], and satellite/drone to ground channels [28], [29]. Therefore, the Rician channel model is adopted in this work.

To resolve the spectral efficiency and SER conflict of MASK, Al-Dweik and Iraqi [1] recently proposed a semi-coherent detection scheme, also denoted as amplitude coherent (AC) detection, that allows using MASK modulation with $M > 2$ over dispersive channels while maintaining the main advantages of noncoherent detection such as receiver low complexity, and immunity to phase noise and frequency offsets. The AC detector requires only the knowledge of the channel gain, which can be obtained blindly and efficiently for single and multicarrier modulation schemes [30]. The channel phase information is not required, which is the main factor that contributes to the complexity reduction of the detector. The optimum, suboptimum and a heuristic detectors are derived in Rayleigh fading channels, and the performance of the heuristic detector is evaluated with and without perfect knowledge of the channel gain in [1] and [30], respectively. The optimum amplitudes of the transmitted MASK symbols are then derived for multibranch detectors in [31]. However, the Rayleigh fading model is limited to wireless applications with no line-of-sight (LoS) signal component. Therefore, applying the AC detector and evaluating its performance in a more general channel model is indispensable.

Consequently, this paper considers applying the AC detection technique to communications system in Rician fading channels with single and multiple receiving antennas. More specifically, the optimum AC detector is derived, and its SER is compared with the optimum coherent and noncoherent MASK detectors. Moreover, the SER of the heuristic detector [1] is derived using two different approaches, and efficient expressions are obtained. One of the approaches results in closed-form SER formula, which is then simplified to provide the asymptotic SER at high SNRs. The other approach results in an efficient expression that contains a single integral. The obtained analytical and simulation results demonstrate that the AC detector can offer reliable SER performance that is comparable to coherent detection

in Rician fading channels.

The rest of the paper is organized as follows. Section II presents the model of M-ary ASK system. In section III, the different types of considered detectors are derived including coherent, non-coherent and amplitude coherent detectors. Sections IV and V present the two approaches considered for analyzing the SER for the heuristic AC detector. Sections VI and VII provide the numerical results and conclusion, respectively.

2 System and Channel Models

In unipolar MASK systems, the baseband representation of the transmitted signal during the ℓth signaling interval is given by

$$d^{\{\ell\}} = s_m,\, m \in \{0,\, 1,\, ...,\, M-1\}, \tag{1}$$

where M is the modulation order, the transmitted symbols $s_m \in \mathbb{R}$, where $\mathbb{R}$ the set of positive real numbers including the 0. Without loss of generality, the symbols' amplitudes can be ordered such that $s_{m+1} > s_m$. Moreover, the amplitude spacing is assumed to be uniform such that $s_{m+1} - s_m = \delta$. It should be noticed that $\frac{1}{M}\sum_{m=0}^{M-1} E_m = 1$, $E_m = s_m^2$ when the average symbol energy is normalized to unity. Therefore, the transmitted symbol during the ℓth transmission interval can be described by,

$$d^{\{\ell\}} = m \times \delta, \quad m \in \{0,\, 1,\, ...,\, M-1\}, \tag{2}$$

where m is selected uniformly, and

$$\delta = \sqrt{\frac{6}{(2M-1)\,(M-1)}}. \tag{3}$$

The system under consideration assumes that the transmitter is equipped with single transmit antenna, and the receiver is equipped with N receiving antennas. The channels between the transmitting and receiving antennas are assumed to be flat, independent and identically distributed (iid) Rician fading channels. Therefore, the received signals in vector notations can be written as

$$\mathbf{r} = \mathbf{h}s_m + \mathbf{n}, \tag{4}$$

where the channel fading vector $\mathbf{h} \in \mathbb{C}^{N\times 1}$, $h_i \sim \mathcal{CN}\left(m_h,\, 2\sigma_h^2\right)$ represents the Rician fading, s_m is the information symbol selected uniformly from the set $\mathbb{S} = \{s_0,\, s_1,\, ...,\, s_{M-1}\}$, and the additive white Gaussian noise (AWGN) vector $\mathbf{n} \in \mathbb{C}^{N\times 1}$ where $n_i \sim \mathcal{CN}\left(0,\, 2\sigma_n^2\right)$. The received signal in (4) can also be written as

$$\mathbf{r} = [\alpha \circ \mathbf{\Phi}]\, s_m + \mathbf{n}, \tag{5}$$

where $\alpha = [|h_1|,\ |h_2|,\ \ldots,\ |h_N|]$, $\mathbf{\Phi} \triangleq e^{j\theta}$, and $\circ$ denotes the Hadamard product.

2.1 Rician Channel Model

In Rician fading, the received signal has a LoS component that affects the received signal envelope and phase. After dropping the channel index, the joint probability density function (PDF) of the channel envelope $\alpha \triangleq |h|$ and and phase $\theta \triangleq \arg\{h\}$ is given by

$$f\,(\alpha, \theta) = \frac{\alpha}{2\pi\sigma_h^2} \exp\left(-\frac{\alpha^2 - 2\mu_h \alpha \cos\theta + \mu_h^2}{2\sigma_h^2}\right), \tag{6}$$

where $\mu_h = |m_h|$. The marginal PDF of α can be obtained by averaging the joint PDF $f(\alpha, \theta)$ over θ. Thus

$$f(\alpha) = \int_{-\pi}^{\pi} f(\alpha, \theta)\ d\theta \tag{7}$$

$$= \frac{2(1+K)}{\Omega} \alpha\, \mathrm{e}^{-K}\, \mathrm{e}^{-\frac{(1+K)}{\Omega}\alpha^2}\ I_0\left(2\alpha\sqrt{\frac{K(1+K)}{\Omega}}\right), \tag{8}$$

where $\Omega = \mu_h^2 + 2\sigma_h^2$ and $K = \frac{\mu_h^2}{2\sigma_h^2}$. Similarly, the PDF of the phase θ can be obtained by averaging over the PDF of α [32], which gives

$$f(\theta) = \frac{1}{2\pi}\exp\left(-\frac{\mu_h^2}{2\sigma_h^2}\right) + \frac{\mu_h \cos(\theta+\phi)}{\sqrt{2\pi}\sigma_h}\exp\left(\frac{-\mu_h^2}{2\sigma_h^2}\sin^2(\theta+\phi)\right) Q\left(-\frac{\mu_h}{\sigma_h}\cos(\theta+\phi)\right), \tag{9}$$

where $\phi = \tan^{-1}\left(\frac{\mu_{h,Q}}{\mu_{h,I}}\right)$, $\mu_{h,I} \triangleq \Re\{m_h\}$ and $\mu_{h,Q} = \Im\{m_h\}$.

3 MASK Detector Design

Usually, there is a trade-off between the receiver complexity and SER performance. The complexity may refer to the computational complexity, hardware complexity or the amount of information required at the receiver side. Adopting a certain detector design depends on the desired application. Other parameters such as the spectral efficiency can affect the complexity and SER. Because it is typically difficult to achieve such conflicting objectives simultaneously, it is crucial to have various options that may fit various applications. In this section, various optimum and suboptimum detectors are derived for MASK signals in Rician fading channels, and their complexity will be discussed.

3.1 Coherent Detection

Based on the signal model in (4), and noting that all received N signals are mutually independent, the conditional PDF of $\mathbf{r}$ for a given fading vector $\mathbf{h}$, and a transmitted symbol s_m is given by [40]

$$f(\mathbf{r}|\mathbf{h},s_m) = \prod_{i=1}^{N} f(r_i|h_i,s_m). \tag{10}$$

As can be noted from (4), $f(r_i|h_i,s_m) \sim \mathcal{CN}\left(h_i s_m, 2\sigma_n^2\right)$, and thus

$$f(\mathbf{r}|\mathbf{h},s_m) = \prod_{i=1}^{N} f(r_i|h_i,s_m)$$

$$= \frac{1}{(2\pi\sigma_n^2)^N}\prod_{i=1}^{N}\exp\left(-\frac{1}{2\sigma_n^2}|r_i - h_i s_m|^2\right). \tag{11}$$

The maximum likelihood (ML) detector based on (11) can be formulated as

$$\hat{d} = \arg\max_{\tilde{s}_m \in \mathbb{S}}\ f(\mathbf{r}|\mathbf{h},\tilde{s}_m) \tag{12}$$

which gives after taking the log of the objective function, dropping the common terms and constants,

$$\hat{d} = \arg\min_{\tilde{s}_m \in \mathbb{S}} \sum_{i=1}^{N} |r_i - h_i \tilde{s}_m|^2. \tag{13}$$

As can be noted from (13), the computational complexity of the coherent detector is low, however, the fading parameters represented by $\mathbf{h}$ should be estimated. Generally speaking, estimating $\mathbf{h}$ requires significant efforts, and inaccurate channel estimation deteriorates the system SER [33].

3.2 Noncoherent Detection

The noncoherent detector can be derived following the same approach of the coherent detector, except that the detector should not have any information about the instantaneous values of $\mathbf{h}$. Consequently, $\mathbf{h}$ should be treated as a random vector. In such cases, the ML detector can be formulated as

$$\begin{aligned}\hat{d} &= \arg\max_{\tilde{s}_m \in \mathbb{S}} \; f\left(\mathbf{r}|\tilde{s}_m\right) \\ &= \arg\max_{\tilde{s}_m \in \mathbb{S}} \; \prod_{i=1}^{N} f(r_i|\tilde{s}_m). \end{aligned} \tag{14}$$

The conditional PDF $f\left(r_i|s_m\right)$ is the sum of two complex Gaussian random variables and thus

$$f\left(r_i|s_m\right) = \frac{1}{\pi\sigma_{\mathrm{r}}^2} \exp\left(-\frac{\left|r_i - \mu_h s_m\right|^2}{\sigma_{\mathrm{r}}^2}\right). \tag{15}$$

where $\sigma_{\mathrm{r}}^2 \triangleq 2\left(\sigma_h^2 s_m^2 + \sigma_n^2\right)$After some straightforward simplifications, the ML noncoherent detector reduces to

$$\hat{d} = \arg\min_{\tilde{s}_m \in \mathbb{R}} \left\{ -N \ln\left(\pi\tilde{\sigma}_{\mathrm{r}}^2\right) + \frac{1}{\tilde{\sigma}_{\mathrm{r}}^2} \sum_{i=1}^{N} \left|r_i - \mu_h \tilde{s}_m\right|^2 \right\}, \tag{16}$$

where $\tilde{\sigma}_{\mathrm{r}}^2 = \sigma_{\mathrm{r}}^2$ except that s_m is replaced by $\tilde{s}_m$. As can be noted from (16), the noncoherent detector does not require the knowledge of $\mathbf{h}$, instead, it requires the channel statistical information, i.e., the values of μ_h, σ_h^2 and σ_n^2. Estimating the statistical information of the channel is generally challenging because it requires large number of observations, and hence, large delay and high computational complexity. Therefore, similar to the coherent detector, the noncoherent detector has complexity limitations as well.

3.3 Amplitude Coherent Detection

The AC detector is designed such as a compromise between the poor SER of the noncoherent and the high complexity of the coherent detector caused by the channel estimation process [1]. More specifically, the AC detector is designed assuming that the receiver has partial knowledge about the channel, namely, the fading gains vector α, but no information is required for $\mathbf{\Phi}$. Since phase estimation is typically more complex to achieve as compared to the channel envelope, the AC detector complexity is less than the coherent detection [30]. The following subsections present the derivation of the optimum and suboptimum AC detectors.

3.3.1 Optimum AC Detector

The optimum AC detector can be derived by applying the ML criterion and assuming the phase shift introduced by the channel is unknown. Therefore,

$$\hat{d} = \arg\max_{\tilde{s}_m \in \mathbb{S}} \; f\left(\mathbf{r}|\alpha, \tilde{s}_m\right). \tag{17}$$

Because r_i $\forall i$ are mutually independent, then the conditional joint PDF of $\mathbf{r}$ given that only the channel gain α is known, can be derived as

$$f\left(\mathbf{r}|\alpha,s_m\right)=\prod_{i=1}^{N}\int_{-\pi}^{\pi}f\left(r_i|\alpha_i,\theta_i,s_m\right)f_{\theta_i}(\theta_i)d\theta_i, \tag{18}$$

where $f(\theta_i)$ is given in (9). By noting that the real and imaginary parts of r_i are independent, and dropping the index i for notational simplicity, then $f\left(r_i|\alpha_i,\theta_i,s_m\right)$ can be written as

$$\begin{aligned}f\left(r|\alpha,\theta,s_m\right)&=f\left(r_{\Re}|\alpha,\theta,s_m\right)f\left(r_{\Im}|\alpha,\theta,s_m\right)\\&=\frac{1}{2\pi\sigma_n^2}\exp\left[-\frac{|r|^2+\alpha^2s_m^2}{2\sigma_n^2}\right]\exp\left[\frac{\alpha s_m}{\sigma_n^2}\left(r_{\Im}\sin\left(\theta\right)+r_{\Re}\cos\left(\theta\right)\right)\right]\\&=\frac{1}{2\pi\sigma_n^2}\exp\left[-\frac{|r|^2+\alpha^2s_m^2}{2\sigma_n^2}\right]\exp\left[\frac{\alpha s_m}{\sigma_n^2}|r|\cos(\theta-\theta_{\mathrm{r}})\right],\end{aligned} \tag{19}$$

where $\theta_{\mathrm{r}}\triangleq\tan^{-1}\left(r_{\Im}/r_{\Re}\right)$. Then, $f\left(r|\alpha,s_m\right)$ can be evaluated by substituting (9) and (19) into (18).

Because evaluating the integral in (18) is intractable, Von Mises (Tikhonov or circular normal) distribution is used as approximation for $f_\theta(\theta)$ in (9), which can be written as [34]

$$f(\theta)\approx\frac{1}{2\pi I_0\left(2\sqrt{K\left(K+1\right)}\right)}\exp\left(2\sqrt{K\left(K+1\right)}\cos\left(\theta-\phi\right)\right). \tag{20}$$

Therefore, the integral in (18) can be written as

$$f\left(r|\alpha,s_m\right)\approx G\left(r\right)\exp\left(-\frac{\alpha^2s_m^2}{2\sigma_n^2}\right)\mathcal{I}_\theta. \tag{21}$$

where $G\left(r\right)$

$$G\left(r\right)=\frac{1}{2\pi I_0\left(2\sqrt{K\left(K+1\right)}\right)\sigma_n^2}\exp\left(-\frac{|r|^2}{2\sigma_n^2}\right) \tag{22}$$

and

$$\mathcal{I}_\theta=\frac{1}{2\pi}\int_{-\pi}^{\pi}\exp\left(2\sqrt{K\left(K+1\right)}\cos\left(\theta-\phi\right)\right)\exp\left(\frac{\alpha s_m}{\sigma_n^2}|r|\cos\left(\theta-\theta_{\mathrm{r}}\right)\right)d\theta. \tag{23}$$

The factor $G\left(r\right)$ can be considered constant with respect to the maximization process in (17), thus, it is more convenient to separate it from the other terms. Moreover, for the special case where $s_m=0$, the PDF $f\left(r|\alpha,\theta,s_m=0\right)$ is independent of α and θ. Thus,

$$\begin{aligned}f\left(r|\alpha,\theta,s_0=0\right)&=\frac{1}{2\pi\sigma_n^2}\exp\left[-\frac{|r|^2}{2\sigma_n^2}\right]\\&=G\left(r\right)I_0\left(2\sqrt{K\left(K+1\right)}\right).\end{aligned} \tag{24}$$

For $s_m\neq0$, evaluating the integral $\mathcal{I}_\theta$ is actually intractable due to the existence of ϕ and θ_{r}. Moreover, θ_{r} depends nonlinearly on θ, which makes it difficult to evaluate $\mathcal{I}_\theta$ even numerically. To overcome this problem, we assume that θ_{r} is independent of θ, consequently, the derived detector is near-optimal. Moreover, θ_{r} represents the phase of the received signal r_i, and hence it can be computed directly at the receiver. The SER performance of the near-optimal detector is expected to be close to the optimum at low SNRs because the second exponent in (23) will be less significant, and hence, the assumption that θ_{r} and θ are independent will not have substantial effect on the SER. On the contrary, at high SNRs, the second exponent dominates the value of $\mathcal{I}_\theta$, and hence the SER is expected to diverge from the

optimum.

Based on the assumption that θ and θ_{r} are independent, the Gauss-Chebyshev quadrature integration rule can used as shown in Appendix I to derive an approximate solution, which is given by

$$\mathcal{I}_{\theta} = \frac{1}{L}\sum_{l=1}^{L} \exp\left[\left(\bar{K}\cos\left(\phi\right) + \tfrac{\cos(\theta_{\mathrm{r}})}{\sigma_n^2}\alpha s_m\left|r\right|\right)\cos\left(\varphi + \pi\tfrac{2l-1}{2L}\right) + \left(\bar{K}\sin\left(\phi\right) + \tfrac{\sin(\theta_{\mathrm{r}})}{\sigma_n^2}\alpha s_m\left|r\right|\right)\sin\left(\varphi + \pi\tfrac{2l-1}{2L}\right)\right] \tag{25}$$

where $\bar{K} = 2\sqrt{K\left(K+1\right)}$, L is the quadrature order, and

$$\varphi = \tan^{-1}\left(\frac{\bar{K}\sin\left(\phi\right) + \frac{1}{\sigma_n^2}\sin\left(\theta_{\mathrm{r}}\right)\alpha s_m\left|r\right|}{\bar{K}\cos\left(\phi\right) + \frac{1}{\sigma_n^2}\cos\left(\theta_{\mathrm{r}}\right)\alpha s_m\left|r\right|}\right).$$

Therefore, after applying the $\ln\left(\cdot\right)$ function and dropping the common and constant terms, the optimum AC detector reduces to

$$\hat{d} = \arg\min_{\tilde{s}_m\in\mathbb{S}} \sum_{i=1}^{N} \frac{\alpha_i^2\tilde{s}_m^2}{2\sigma_n^2} - \ln\tilde{\mathcal{I}}_{\theta_i} \tag{26}$$

where $\tilde{\mathcal{I}}_{\theta_i} = \mathcal{I}_{\theta_i}|_{s_m\to\tilde{s}_m}$. As can be noted from (26), the optimum AC detector has very high computational complexity induced by $\mathcal{I}_{\theta_i}$, which makes it prohibitively expensive to implement. Moreover, the detector requires the knowledge of the noise variance σ_n^2 and the Rician fading parameter K. The received signal phase can be computed directly from the received signal, $\theta_{\mathrm{r}_i} \triangleq \tan^{-1}\left(r_{i,\Im}/r_{i,\Re}\right)$.

3.3.2 Suboptimum AC Detector

As can be noted from (76) in Appendix I, B and D dominates $g\left(\theta\right)$ at high SNRs, i.e., $B \gg A\cos\left(\phi\right)$ and $D \gg C$. Thus, substituting $A = C = 0$ in (76) yields

$$\begin{aligned}
\mathcal{I}_{\theta} &\approx \frac{1}{2\pi}\int_{-\pi}^{\pi} \exp\left(B\alpha s_m\left|r\right|\cos\left(\theta\right) + D\alpha s_m\left|r\right|\sin\left(\theta\right)\right)d\theta \\
&= \frac{1}{2\pi}\int_{-\pi}^{\pi} \exp\left(\frac{\alpha s_m\left|r\right|}{\sigma_n^2}\cos\left(\theta_{\mathrm{r}}\right)\cos\left(\theta\right) + \frac{\alpha_i s_m\left|r\right|}{\sigma_n^2}\sin\left(\theta_{\mathrm{r}}\right)\sin\left(\theta\right)\right)d\theta \\
&= \frac{1}{2\pi}\int_{-\pi}^{\pi} \exp\left(\frac{\alpha s_m\left|r\right|}{\sigma_n^2}\left(\cos\left(\theta_{\mathrm{r}}\right)\cos\left(\theta\right) + \sin\left(\theta_{\mathrm{r}}\right)\sin\left(\theta\right)\right)\right)d\theta \\
&= \frac{1}{2\pi}\int_{-\pi}^{\pi} \exp\left(\frac{\alpha s_m\left|r\right|}{\sigma_n^2}\cos\left(\theta - \theta_{\mathrm{r}}\right)\right)d\theta \\
&= \frac{1}{\pi}\int_{0}^{\pi} \exp\left(\frac{\alpha s_m\left|r\right|}{\sigma_n^2}\cos\left(\theta\right)\right)d\theta \\
&= I_0\left(\frac{\alpha s_m\left|r\right|}{\sigma_n^2}\right).
\end{aligned} \tag{27}$$

It is worth noting that θ_{r} does not affect the result of the integral because it is only a phase shift. Therefore, the AC detector can be expressed as

$$\hat{d} = \arg\min_{\tilde{s}_m\in\mathbb{S}} \sum_{i=1}^{N} \frac{\alpha_i^2\tilde{s}_m^2}{2\sigma_n^2} - \ln\left[I_0\left(\frac{\alpha_i\tilde{s}_m\left|r_i\right|}{\sigma_n^2}\right)\right]. \tag{28}$$

The suboptimum AC detector described in (28) is similar to the optimum AC detector derived in [1] for Rayleigh fading channels. Although this detector does not require knowledge of the statistical channel information, it requires computing the Bessel function, which incurs high complexity.

Another suboptimal detector can be obtained by directly substituting $A = 0$ and $C = 0$ in (25), therefore $\mathcal{I}_{\theta}$ can

be approximated as

$$\begin{aligned}\mathcal{I}_\theta &\approx \frac{1}{L}\sum_{l=1}^{L}\exp\left[\frac{\alpha s_m\,|r|}{\sigma_n^2}\left(\cos\left(\theta_{\mathrm{r}}\right)\cos\left(\varphi+\pi\tfrac{2l-1}{2L}\right)+\sin\left(\theta_{\mathrm{r}}\right)\sin\left(\varphi+\pi\tfrac{2l-1}{2L}\right)\right)\right]\\ &= \frac{1}{L}\sum_{l=1}^{L}\exp\left[\frac{\alpha s_m\,|r|}{\sigma_n^2}\left(\cos\left(-\pi\tfrac{2l-1}{2L}\right)\right)\right]\\ &= \frac{1}{L}\sum_{l=1}^{L}\exp\left[\frac{\alpha s_m\,|r|}{\sigma_n^2}\cos\left(\pi\tfrac{2l-1}{2L}\right)\right].\end{aligned} \tag{29}$$

Interestingly, this approach does not contain the Bessel function.

3.3.3 Heuristic ACD (HACD)

Although the two suboptimum AC detectors derived above are less complex than the optimum AC detector, evaluating the Bessel and exponential functions is necessary to calculate the decision metric. Therefore, the heuristic detector presented in [1] is considered to reduce the complexity even further. The heuristic detector is given by

$$\hat{d} = \arg\min_{\tilde{s}_m\in\mathbb{S}}\ \left[\zeta-\tilde{s}_m^2\right]^2, \tag{30}$$

where ζ is the combined signal from the N antennas, which is given by

$$\zeta = \frac{|r|_\Sigma^2}{\sum_{i=1}^{N}\alpha_i^2}, \tag{31}$$

where $|r|_\Sigma^2 = \sum_{i=1}^{N}|r_i|^2$. For SER analysis, it is more convenient to express (30) as

$$\hat{d} = \begin{cases} s_0, & 0<\zeta<\eta_{0,1}\\ s_1, & \eta_{0,1}<\zeta<\eta_{1,2}\\ \vdots & \vdots\\ s_{M-1}, & \eta_{M-1,M-2}<\zeta<\infty\end{cases}, \tag{32}$$

where $\eta_{i,j}$'s are the detection thresholds and given by

$$\eta_{i,j} = \frac{s_i^2+s_j^2}{2}. \tag{33}$$

In the following two sections, two different approaches are presented to evaluate the SER analytically.

4 Approach I: SER Analysis of the Heuristic AC Detector

Based on (32), the SER P_e for the heuristic AC detector can be written as,

$$\begin{aligned}P_e &= 1-\frac{1}{M}\left(\int_0^{\eta_{0,1}} f\left(\zeta|E_0\right)d\zeta+\int_{\eta_{M-2,M-1}}^{\infty} f\left(\zeta|E_{M-1}\right)d\zeta+\sum_{m=1}^{M-2}\int_{\eta_{m,m-1}}^{\eta_{m,m+1}} f\left(\zeta|E_m\right)d\zeta\right)\\ &= 1-\frac{1}{M}\left(F_\zeta\left(\eta_{0,1}|E_0\right)+1-F_\zeta\left(\eta_{M-2,M-1}|E_{M-1}\right)+\sum_{m=1}^{M-2}F_\zeta\left(\eta_{m,m+1}|E_m\right)-F_\zeta\left(\eta_{m,m-1}|E_m\right)\right)\end{aligned} \tag{34}$$

where F_ζ is the cumulative distribution function (CDF), which typically can be evaluated as

$$F_\zeta\left(\zeta|E_m\right)=\int_0^\zeta\int_0^\infty\cdots\int_0^\infty f\left(\zeta|\alpha,E_m\right)f\left(\alpha\right)d\alpha\ d\zeta. \tag{35}$$

However, the N-fold integral in (35) can be substantially simplified by noting that $f\left(\zeta|\alpha,E_m\right)$ is actually a function of $\sum_{i=1}^N\alpha_i^2\triangleq x$. Consequently, the integral reduces to

$$F_\zeta\left(\zeta|E_m\right)=\int_0^\zeta\int_0^\infty f\left(\zeta|x,E_m\right)f\left(x\right)dx\ d\zeta, \tag{36}$$

The PDF of x can be derived by noting that $h_i\sim\mathcal{CN}\left(m_h,2\sigma_h^2\right)$, thus $f\left(x\right)$ is noncentral Chi-squared

$$f\left(x\right)=\frac{\exp\left(-\frac{\lambda}{2}\right)}{2\sigma_h^2}\exp\left(-\frac{x}{2\sigma_h^2}\right)\left(\frac{x}{\lambda\sigma_h^2}\right)^{0.5(N-1)}I_{N-1}\left(\sqrt{\frac{\lambda}{\sigma_h^2}x}\right), \tag{37}$$

where

$$\begin{aligned}\lambda&=\sum_{i=1}^N\mu_{h_I}^2+\mu_{h_Q}^2\\&=\sum_{i=1}^N\frac{\mu_h^2\cos^2\phi}{\sigma_h^2}+\frac{\mu_h^2\sin^2\phi}{\sigma_h^2}\\&=2KN.\end{aligned} \tag{38}$$

and the complete derivation can be found in Appendix II. To derive $f\left(\zeta|x,E_m\right)$ of the Heuristic detector (30), the decision variable can be written as

$$\begin{aligned}\zeta&=\frac{|r|_\Sigma^2}{\sum_{i=1}^N\alpha_i^2}\\&=\frac{1}{\sum_{i=1}^N\alpha_i^2}\sum_{i=1}^N|r_i|^2\\&=\frac{1}{\sum_{i=1}^N\alpha_i^2}\underbrace{\sum_{i=1}^N|r_{i,\Re}+jr_{i,\Im}|^2}_{r_T},\end{aligned} \tag{39}$$

where $r_{i,\Re}=\alpha_i s_m\cos\left(\theta_i\right)+n_{i,\Re}$ and $r_{i,\Im}=\alpha_i s_m\sin\left(\theta_i\right)+n_{i,\Im}$. By noting that $r_{i,\Re}$ and $r_{i,\Im}$ are mutually independent $\forall i$, and the PDF for each of which is conditionally Gaussian, i.e., $f\left(r_{i,\Re}|\alpha_i,s_m,\cos\left(\theta_i\right)\right)\sim\mathcal{N}\left(\alpha_i s_m\cos\left(\theta_i\right),\sigma_n^2\right)$ and $f\left(r_{i,\Im}|\alpha_i,s_m,\sin\left(\theta_i\right)\right)\sim\mathcal{N}\left(\alpha_i s_m\sin\left(\theta_i\right),\sigma_n^2\right)$. Therefore, $f\left(|r_i|^2|\alpha_i,s_m,\theta_i\right)$is conditionally noncentral Chi-squared with two degrees of freedom and noncentrality factor λ_i, i.e., $f\left(|r_i|^2|\alpha_i,s_m,\theta_i\right)\sim\chi^2\left(2,\lambda_i\right)$, where

$$\begin{aligned}\lambda_i&=\left[\alpha_i s_m\cos\left(\theta_i\right)\right]^2+\left[\alpha_i s_m\cos\left(\theta_i\right)\right]^2\\&=\alpha_i^2 s_m^2.\end{aligned} \tag{40}$$

Therefore, $f\left(|r_i|^2|\alpha_i,s_m,\theta_i\right)=f\left(|r_i|^2|\alpha_i,s_m\right)\sim\chi^2\left(2,\lambda_i\right)$. Therefore, $f\left(\zeta|x\right)$ can be written as

$$f\left(\zeta|x,E_m\right)=\frac{x}{2\sigma_n^2}\left(\frac{\zeta}{E_m}\right)^{0.5(N-1)}\exp\left(-x\frac{\zeta+E_m}{2\sigma_n^2}\right)I_{N-1}\left(\frac{x}{\sigma_n^2}\sqrt{E_m\zeta}\right),\ m>0. \tag{41}$$

For the case of $m=0$, $r_{i,\Re}=n_{i,\Re}\sim\mathcal{N}\left(0,\sigma_n^2\right)$ and $r_{i,\Im}=n_{i,\Im}\sim\mathcal{N}\left(0,\sigma_n^2\right)$, thus, $f\left(|r_i|^2\,|\alpha_i,d_m,\theta_i\right)=f\left(|r_i|^2\right)$ which has exponential PDF with parameter $\beta=2\sigma_n^2$. Consequently, the PDF of the sum of N iid exponential random variables is Erlang distribution, i.e.,

$$f\left(\zeta|x\right)=\frac{\lambda_0^N}{(N-1)!}x^N\ \zeta^{N-1}\exp\left(-\lambda_0\zeta x\right),\ m=0. \tag{42}$$

where $\lambda_0=\frac{1}{2\sigma_n^2}$.

4.1 Evaluating $F_\zeta\left(\zeta|E_m\right)$, $m>0$

To simplify the analysis, we replace the Bessel function in (37) by its series expansion [35], which gives

$$I_{N-1}\left(\sqrt{\frac{\lambda}{\sigma_h^2}x}\right)=\sum_{l=0}^{\infty}\frac{1}{l!\Gamma\left(l+N\right)}\left(\frac{\lambda}{4\sigma_h^2}\right)^{\frac{2l+N-1}{2}}(x)^{\frac{2l+N-1}{2}}. \tag{43}$$

Although the same series expansion can be used to represent the Bessel function in (41), the argument of the Bessel function $\sqrt{\frac{E_m\ \zeta}{\sigma_n^2}}x\gg1$ for most typical values of σ_n^2. Therefore, the following approximation can be used [36],

$$I_{N-1}\left(\frac{x}{\sigma_n^2}\sqrt{E_m\zeta}\right)\simeq\frac{\exp\left(\frac{x\sqrt{E_m\ \zeta}}{\sigma_n^2}\right)}{\sqrt[4]{E_m\ \zeta}\sqrt{\frac{2\pi}{\sigma_n^2}x}}\left(1+\sum_{q=1}^{Q}\left(\frac{(-1)^q}{x^q}\frac{\prod_{k=1}^{q}\left[4\left(N-1\right)^2-\left(2k-1\right)^2\right]}{q!8^q\left(\frac{\sqrt{E_m\zeta}}{\sigma_n^2}\right)^q}\right)\right). \tag{44}$$

Using (43) and (44), and noting that

$$f\left(\zeta|E_m\right)=\int_0^{\infty}f\left(\zeta|x,E_m\right)\ f\left(x\right)dx, \tag{45}$$

the PDF $f\left(\zeta|E_m\right)$ after evaluating the integral, as depicted in Appendix II, is given by

$$f\left(\zeta|E_m\right)=C\ \left(\sum_{l=0}^{\infty}A_l\zeta^{\ 0.5N-0.75}\ C_\zeta^{-(l+N+0.5)}+\sum_{q=1}^{Q}\sum_{l=0}^{L}B_q^l\ \zeta^{0.5N-0.5q-0.75}\ C_\zeta^{-(N-q+l+0.5)}\right),\ m>0 \tag{46}$$

where the variables C, C_ζ, A_l and B_q^l are given by

$$C_\zeta\triangleq\frac{\zeta+E_m}{2\sigma_n^2}+\frac{\sigma_h^2}{2}-\frac{\sqrt{E_m\ \zeta}}{\sigma_n^2} \tag{47}$$

$$C=\frac{\exp\left(-\frac{\lambda}{2}\right)}{4\sigma_n^2\sigma_h^2}\left(\frac{1}{E_m\sigma_h^2\lambda}\right)^{0.5(N-1)}\frac{1}{\sqrt{2\pi\frac{\sqrt{E_m}}{\sigma_n^2}}} \tag{48}$$

$$A_l=\frac{\Gamma\left(l+N+0.5\right)}{l!\Gamma\left(l+N\right)}\left(\frac{\lambda}{4\sigma_h^2}\right)^{\frac{2l+N-1}{2}} \tag{49}$$

$$B_q^l=\frac{\Gamma\left(N-q+l+0.5\right)}{l!\Gamma\left(l+N\right)}\left(\frac{\lambda}{4\sigma_h^2}\right)^{\frac{2l+N-1}{2}}\left((-1)^q\frac{\prod_{k=1}^{q}\left[4\left(N-1\right)^2-\left(2k-1\right)^2\right]}{q!8^q\left(\frac{\sqrt{E_m}}{\sigma_n^2}\right)^q}\right), \tag{50}$$

where $\Gamma\left(\cdot\right)$ is the Gamma function [35].

Finally, the CDF $F_\zeta(\zeta|E_m)$, $m>0$ can be evaluated as

$$\begin{aligned} F_\zeta(\zeta|E_m) &= \int_0^\zeta f\left(\acute{\zeta}|E_m\right) d\acute{\zeta} \\ &= C\left(\sum_{l=0}^{\infty} A_l \mathcal{I}_A^l + \sum_{q=1}^{Q}\sum_{l=0}^{\infty} B_m^l \mathcal{I}_B^{q,l}\right),\ m>0, \end{aligned} \tag{51}$$

where $\mathcal{I}_A^l$ and $\mathcal{I}_B^{q,l}$ are given by

$$\mathcal{I}_A^l = 2\int_0^{\sqrt{\zeta}} y^{2(0.5N-0.75)+1}\left(\frac{y^2}{2\sigma_n^2} - \frac{\sqrt{E_m}}{\sigma_n^2}y + c\right)^{-(l+N+0.5)} dy \tag{52}$$

$$\mathcal{I}_B^{q,l} = 2\int_0^{\sqrt{\zeta}} y^{2(0.5N-0.5q-0.75)+1}\left(\frac{y^2}{2\sigma_n^2} - \frac{\sqrt{E_m}}{\sigma_n^2}y + c\right)^{-(N-q+l+0.5)} dy, \tag{53}$$

where $c = \frac{1}{2\sigma_h^2} + \frac{E_m}{2\sigma_n^2}$.

4.2 Evaluating $F_\zeta(\zeta|E_m)$, $m=0$

Averaging $\mathrm{f}(\zeta|x,E_m)$ over $\mathrm{f}(x)$ using series expansion of the Bessel function using (43) yields

$$\begin{aligned} f(\zeta|E_m) &= \int_0^\infty \mathrm{f}(\zeta|x,E_m)\ \ f(x)\,dx \\ &= C_0\ \zeta^{N-1}\sum_{l=0}^{\infty}\frac{\Gamma(2N+l)}{l!\Gamma(l+N)}\left(\frac{\lambda_0}{4\sigma_h^2}\right)^{\frac{2l+N-1}{2}}\left(\lambda_0\zeta + \frac{1}{2\sigma_h^2}\right)^{-(2N+l)},\ m=0 \end{aligned} \tag{54}$$

where C_0 is given by

$$C_0 = \frac{\lambda_0^N}{(N-1)!}\frac{1}{2\sigma_h^2}\left(\frac{1}{\lambda_0\sigma_h^2}\right)^{0.5(N-1)}\exp\left(-\frac{\lambda_0}{2}\right). \tag{55}$$

The complete derivation of $f(\zeta|E_m)$ is given in Appendix III.

Finally, the CDF of ζ can be evaluated as

$$\begin{aligned} F_\zeta(\zeta|E_m) &= \int_0^\zeta f\left(\acute{\zeta}|E_m\right) d\acute{\zeta} \\ &= C_0\sum_{l=0}^{\infty}\frac{\Gamma(2N+l)}{l!\Gamma(l+N)}\left(\frac{\lambda_0}{4\sigma_h^2}\right)^{\frac{2l+N-1}{2}}\int_0^\zeta \acute{\zeta}^{N-1}\left(\lambda_0\ \acute{\zeta} + \frac{1}{2\sigma_h^2}\right)^{-(2N+l)} d\acute{\zeta},\ m=0. \end{aligned} \tag{56}$$

It should be noticed that integrals of the form given in (52), (53) and (56) can be solved in recursive manner according to [35, 2.17, page 78].

5 Approach II: Symbol Error Rate Analysis

In the first approach, we used the conditional PDF $f(\zeta|x,E_m)$ to derive the unconditional PDF $f(\zeta|E_m)$, which was used to derive the unconditional CDF. In this part, we derive the conditional CDF $F_\zeta(\zeta|x,E_m)$ from the conditional PDF $f(\zeta|x,E_m)$, and then we derive the unconditional CDF $F_\zeta(\zeta|E_m)$.

By noting that $\zeta = \frac{|r|_\Sigma^2}{x}$, then the conditional PDF $f(\zeta|x,E_m)$ follows an noncentral Chi-squared with $2N$ degrees of freedom, noncentrality parameter E_m, and the variance of Gaussian components is $\frac{\sigma_n^2}{x}$, i.e., $f(\zeta|x,E_m) \sim$

$\chi^2\left(2N, s_m^2\right) = \chi^2\left(2N, E_m\right)$. Thus, $F_\zeta\left(\zeta|x, E_m\right)$ [37] can be defined as

$$F_\zeta\left(\zeta|x, E_m\right) = 1 - Q_N\left(\sqrt{\frac{xE_m}{\sigma_n^2}}, \sqrt{\frac{x\zeta}{\sigma_n^2}}\right). \tag{57}$$

The CDF of ζ given E_m can be calculated by averaging the conditional CDF $F\left(\zeta|x, E_m\right)$ over the distribution of x which is given by

$$F\left(\zeta|E_m\right) = \int_0^\infty F\left(\zeta|x, E_m\right) f(x) dx, \tag{58}$$

where $f(x)$ is given in (37).

5.1 The CDF $F_\zeta(\zeta|E_m)$ for $\zeta < E_m$

The series representation of the generalized Marcum Q-function is given in [38] as

$$Q_v(a, b) = 1 - \sum_{n=0}^{\infty} (-1)^n \exp\left(-\frac{a^2}{2}\right) \frac{L_n^{(v-1)}\left(\frac{a^2}{2}\right)}{\Gamma(v+n+1)} \left(\frac{b^2}{2}\right)^{n+v}, \quad \{a, v\} > 0 \text{ and } b \geq 0 \tag{59}$$

where $L_n^{(\alpha)}(x) = \sum_{k=0}^{n} \frac{\Gamma(n+\alpha+1)}{\Gamma(k+\alpha+1)\Gamma(n-k+1)} \frac{(-x)^k}{k!}$ is the generalized Laguerre polynomial of degree n and order α. Using this formula, the conditional CDF $F\left(\zeta|x, E_m\right)$ can be rewritten as

$$F_\zeta\left(\zeta|x, E_m\right) = \sum_{n=0}^{\infty} \sum_{k=0}^{n} \binom{N+n-1}{N+k-1} \frac{(-1)^{n+k}}{(N+n)!k!} \left(\frac{\zeta}{2\sigma_n^2}\right)^{N+n} \left(\frac{E_m}{2\sigma_n^2}\right)^k x^{N+n+k} \exp\left(-\frac{E_m}{2\sigma_n^2} x\right). \tag{60}$$

Then, the CDF $F_\zeta(\zeta|E_m)$ can be computed as

$$F_\zeta(\zeta|E_m) = \sum_{n=0}^{\infty} \sum_{k=0}^{n} \binom{N+n-1}{N+k-1} \frac{(-1)^{n+k}}{(N+n)!k!} \left(\frac{\zeta}{2\sigma_n^2}\right)^{N+n} \left(\frac{E_m}{2\sigma_n^2}\right)^k \underbrace{\int_0^\infty x^{N+n+k} e^{-\frac{E_m}{2\sigma_n^2} x} f(x) dx}_{A}. \tag{61}$$

The integration A can be solved by [39, Eq. 2.15.5]

$$\begin{aligned} A &= 2\bar{K} \mathrm{e}^{-NK} \left(\frac{\bar{K}}{NK}\right)^{\frac{N-1}{2}} \int_0^\infty \alpha^{2(N+n+k)+N} \exp\left(-\left(\frac{E_m}{2\sigma_n^2} + \bar{K}\right)\alpha^2\right) I_{N-1}\left(2\sqrt{NK\bar{K}}\alpha\right) d\alpha \\ &= \mathrm{e}^{-NK} \bar{K}^N \frac{\Gamma(n+k+2N)}{\Gamma(N)} \left(\frac{E_m}{2\sigma_n^2} + \bar{K}\right)^{-(n+k+2N)} {}_1F_1\left(n+k+2N; N; \frac{NK(1+K)}{1+K+\frac{\Omega}{2\sigma_n^2}E_m}\right), \end{aligned} \tag{62}$$

which can be simplified to

$$\begin{aligned} A &= \frac{e^{-\frac{\lambda}{2}}}{\sigma_h^2} \left(\frac{1}{\lambda\sigma_h^2}\right)^{\frac{N-1}{2}} \int_0^\infty \alpha^{2(N+n+k)+N} \exp\left(-\left(\frac{E_m}{2\sigma_n^2} + \frac{1}{2\sigma_h^2}\right)\alpha^2\right) I_{N-1}\left(\sqrt{\frac{\lambda}{\sigma_h^2}}\alpha\right) d\alpha \\ &= e^{-\frac{\lambda}{2}} \left(\frac{1}{2\sigma_h^2}\right)^N \frac{\Gamma(n+k+2N)}{\Gamma(N)} \left(\frac{E_m}{2\sigma_n^2} + \frac{1}{2\sigma_h^2}\right)^{-(n+k+2N)} {}_1F_1\left(n+k+2N; N; \frac{\lambda}{2\left(1+\frac{\sigma_h^2}{\sigma_n^2}E_m\right)}\right), \end{aligned} \tag{63}$$

where $\bar{K} = \frac{1+K}{\Omega}$ and ${}_1F_1(a; b; z)$ is the confluent hypergeometric function of the first kind.

Consequently, by substituting A into (61) and applying some manipulations, the CDF can be expressed as

$$F_\zeta(\zeta|E_m) = \sum_{n=0}^{\infty}\sum_{k=0}^{n}\binom{N+n-1}{N+k-1}\frac{(-1)^{n+k}(n+k+2N-1)!}{(N-1)!(N+n)!k!}\left(\frac{\zeta}{E_m}\right)^{n+N}\left(K_m\mathrm{e}^{-K}\right)^N \times \frac{\left(\frac{\Omega}{2\sigma_n^2}\right)^{n+k+N}}{\left(\frac{\Omega}{2\sigma_n^2}+K_m\right)^{n+k+2N}}{}_1F_1\left(n+k+2N;N;\frac{NKK_m}{\frac{\Omega}{2\sigma_n^2}+K_m}\right), \quad (64)$$

where $K_m = \frac{1+K}{E_m}$. Note that $\left(\frac{\zeta}{E_m}\right)^n$ in the CDF expression is converged only with $\frac{\zeta}{E_m} < 1$ when n goes to infinity. Therefore, it will be used to calculate the error probability for $\Pr\left(\zeta \le \frac{E_m+E_{m-1}}{2}\right)$.

For high SNR regime, when $\frac{\Omega}{2\sigma_n^2} \to \infty$, (64) can be expressed as

$$\lim_{\frac{\Omega}{2\sigma_n^2}\to\infty}\left(\frac{\frac{\Omega}{2\sigma_n^2}}{\frac{\Omega}{2\sigma_n^2}+K_m}\right)^{n+k+N}{}_1F_1\left(n+k+2N;N;\frac{NKK_m}{\frac{\Omega}{2\sigma_n^2}+K_m}\right) = 1.$$

Then, (64) can be simplified as

$$\begin{aligned} F^{\infty}(\zeta|E_m) &= \left(\frac{K_m e^{-K}}{\frac{\Omega}{2\sigma_n^2}+K_m}\right)^N \sum_{n=0}^{\infty}\left(\frac{\zeta}{E_m}\right)^{n+N}\sum_{k=0}^{n}\binom{N+n-1}{N+k-1}\frac{(-1)^{n+k}(n+k+2N-1)!}{(N-1)!(N+n)!k!} \\ &\overset{(a)}{=} \left(\frac{K_m e^{-K}}{\frac{\Omega}{2\sigma_n^2}+K_m}\right)^N \sum_{n=0}^{\infty}\left(\frac{\zeta}{E_m}\right)^{n+N}\frac{(2N+n-1)!}{n!N!(N-1)!} \\ &\overset{(b)}{=} \binom{2N-1}{N}\left(\frac{K_m e^{-K}}{\frac{\Omega}{2\sigma_n^2}+K_m}\frac{\frac{\zeta}{E_m}}{\left(\frac{\zeta}{E_m}-1\right)^2}\right)^N, \ (\zeta < E_m) \end{aligned} \quad (65)$$

where (a) comes from

$$\sum_{k=0}^{n}(-1)^{n+k}\binom{N+n-1}{N+k-1}\frac{(n+k+2N-1)!}{k!} = \frac{(n+2N-1)!(n+N)!}{n!N!}$$

and (b) comes from

$$\sum_{n=0}^{\infty}a^n\frac{(n+2N-1)!}{n!} = (a-1)^{-2N}(2N-1)!,\ a<1.$$

5.2 The CDF $F_\zeta(\zeta|E_m)$ for $\zeta > E_m$

To evaluate the required CDF, the following relation between $Q_m(a,b)$ and $Q_m(b,a)$ is applied.

$$Q_m(a,b) + Q_m(b,a) = 1 + e^{-\frac{a^2+b^2}{2}}\sum_{k=1-m}^{m-1}\left(\frac{a}{b}\right)^k I_k(ab). \quad (66)$$

Using this transformation, the CDF $F_\zeta(\zeta|x,E_m)$ for $\zeta > E_m$ can be now rewritten as

$$F_\zeta(\zeta|x,E_m) = Q_N\left(\sqrt{\frac{x\zeta}{\sigma_n^2}},\sqrt{\frac{xE_m}{\sigma_n^2}}\right) - \exp\left(-\frac{\zeta+E_m}{2\sigma_n^2}x\right)\sum_{k=1-N}^{N-1}\left(\sqrt{\frac{E_m}{\zeta}}\right)^k I_k\left(\frac{\sqrt{E_m\zeta}}{\sigma_n^2}x\right). \quad (67)$$

The CDF of $F_\zeta(\zeta|E_m)$ can be calculated as

$$F_\zeta(\zeta|E_m) = \underbrace{\int_0^\infty Q_m\left(\sqrt{\tfrac{x\zeta}{\sigma_n^2}}, \sqrt{\tfrac{xE_m}{\sigma_n^2}}\right) f(x)dx}_{B} - \underbrace{\sum_{k=1-N}^{N-1} \left(\sqrt{\tfrac{E_m}{\zeta}}\right)^k \int_0^\infty \exp\left(-\tfrac{\zeta+E_m}{2\sigma_n^2}x\right) I_k\left(\tfrac{\sqrt{E_m\zeta}}{\sigma_n^2}x\right) f(x)dx}_{\acute{C}}, \quad (68)$$

where integrals B and $\acute{C}$ can be evaluated as shown below in (69) and (70), respectively. Integration in B can be calculated similarly as (64) which is given by

$$B = 1 - \sum_{n=0}^{\infty}\sum_{k=0}^{n} \binom{N+n-1}{N+k-1} \frac{(-1)^{n+k}(n+k+2N-1)!}{(N-1)!(N+n)!k!} \left(\frac{E_m}{\zeta}\right)^{n+N} \left(K_\zeta \mathrm{e}^{-K}\right)^N \frac{\left(\frac{\Omega}{2\sigma_n^2}\right)^{n+k+N}}{\left(\frac{\Omega}{2\sigma_n^2}+K_\zeta\right)^{n+k+2N}} \times {}_1F_1\left(n+k+2N; N; \frac{NKK_\zeta}{\frac{\Omega}{2\sigma_n^2}+K_\zeta}\right), \quad (69)$$

where $K_\zeta = \frac{1+K}{\zeta}$.

Using the series representation of modified Bessel function of the first kind, i.e.,

$$I_v(z) = \left(\frac{z}{2}\right)^v \sum_{n=0}^{\infty} \frac{\left(z^2/4\right)^n}{n!(n+v)!}$$

and noting that $I_v(z) = I_{-v}(z)$, the integral $\acute{C}$ can be calculated as

$$\begin{aligned}
\acute{C} &= \sum_{n=0}^{\infty}\sum_{k=1-N}^{N-1} \left(\frac{E_m}{\zeta}\right)^k \frac{\left(\frac{\sqrt{E_m\zeta}}{2\sigma_n^2}\right)^{2n+|k|}}{n!(n+|k|)!} \int_0^\infty x^{2n+|k|} \exp\left(-\frac{\zeta+E_m}{2\sigma_n^2}x\right) f(x)dx \\
&= \sum_{n=0}^{\infty}\sum_{k=1-N}^{N-1} \left(\frac{E_m}{\zeta}\right)^k \frac{\left(\frac{\sqrt{E_m\zeta}}{2\sigma_n^2}\right)^{2n+|k|}}{n!(n+|k|)!} \frac{(2n+|k|+N-1)!}{(N-1)!} e^{-NK} \left(\frac{1}{2\sigma_h^2}\right)^N \\
&\times \left(\frac{\zeta+E_m}{2\sigma_n^2}+\frac{1}{2\sigma_h^2}\right)^{-(2n+|k|+N)} {}_1F_1\left(2n+|k|+N; N; \frac{\lambda}{2\left(1+\frac{\sigma_h^2}{\sigma_n^2}(E_m+\zeta)\right)}\right) \\
&= \sum_{n=0}^{\infty}\sum_{k=1-N}^{N-1} \left(\frac{\sqrt{E_m\zeta}}{E_m+\zeta}\right)^{2n+|k|} \left(\frac{E_m}{\zeta}\right)^k \frac{(2n+|k|+N-1)!}{n!(n+|k|)!(N-1)!} \left(e^{-K}K_{m\zeta}\right)^N \frac{\left(\frac{\Omega}{2\sigma_n^2}\right)^{2n+|k|}}{\left(\frac{\Omega}{2\sigma_n^2}+K_{m\zeta}\right)^{2n+|k|+N}} \\
&\times {}_1F_1\left(2n+|k|+N; N; \frac{NKK_{m\zeta}}{\frac{\Omega}{2\sigma_n^2}+K_{m\zeta}}\right), \quad (70)
\end{aligned}$$

where $K_{m\zeta} = \frac{1+K}{E_m+\zeta}$.It can be noticed that $\left(\frac{E_m}{\zeta}\right)^n$ in this CDF expression is converged only with $\frac{E_m}{\zeta} < 1$ when n goes to infinity. Therefore, it will be used to calculate the error probability for $\Pr\left(\zeta \geq \frac{E_m+E_{m+1}}{2}\right)$.

Similar to the case for $\zeta < E_m$, B and C for $\zeta > E_m$ can be asymptotically represented as

$$B^\infty = 1 - \binom{2N-1}{N} \left(\frac{K_\zeta e^{-K}}{\frac{\Omega}{2\sigma_n^2}+K_\zeta} \cdot \frac{\frac{E_m}{\zeta}}{\left(\frac{E_m}{\zeta}-1\right)^2}\right)^N \quad (71)$$

and

$$\acute{C}^{\infty} = \left(\frac{K_{m\zeta}e^{-K}}{\frac{\Omega}{2\sigma_n^2}+K_{m\zeta}}\right)^N \sum_{k=1-N}^{N-1}\left(\frac{\sqrt{E_m\zeta}}{E_m+\zeta}\right)^{|k|}\left(\frac{E_m}{\zeta}\right)^k \sum_{n=0}^{\infty}\frac{(2n+|k|+N-1)!}{n!(n+|k|)!(N-1)!}\left(\frac{\sqrt{E_m\zeta}}{E_m+\zeta}\right)^{2n}$$
$$= \left(\frac{K_{m\zeta}e^{-K}}{\frac{\Omega}{2\sigma_n^2}+K_{m\zeta}}\right)^N \sum_{k=1-N}^{N-1}\binom{N+|k|-1}{N-1}\left(\frac{\sqrt{E_m\zeta}}{E_m+\zeta}\right)^{|k|}\left(\frac{E_m}{\zeta}\right)^k$$
$$\times\, {}_2F_1\left(\frac{|k|+N}{2},\frac{|k|+N+1}{2},|k|+1,\frac{4E_m\zeta}{(E_m+\zeta)^2}\right). \tag{72}$$

5.3 The CDF for $E_m = 0$ when $\zeta > E_m$

As the CDF in (68) is not valid for E_0, the CDF $F_\zeta(\zeta|E_0)$ is derived separately. Towards this end, the conditional CDF given x can be rewritten as

$$F_\zeta(\zeta|x,E_0) = 1 - Q_N\left(0,\sqrt{\frac{\zeta x}{\sigma_n^2}}\right)$$
$$= 1 - \frac{\Gamma\left(N,\frac{\zeta x}{2\sigma_n^2}\right)}{\Gamma(N)}$$
$$= 1 - \exp\left(-\frac{\zeta x}{2\sigma_n^2}\right)\sum_{k=0}^{N-1}\frac{\left(\frac{\zeta x}{2\sigma_n^2}\right)^k}{k!}. \tag{73}$$

The unconditional CDF is computed as

$$F_\zeta(\zeta|E_0) = 1 - \sum_{k=0}^{N-1}\frac{\left(\frac{\zeta}{2\sigma_n^2}\right)^k}{k!}\int_0^\infty x^k\exp\left(-\frac{\zeta x}{2\sigma_n^2}\right)f(x)dx$$
$$= 1 - \sum_{k=0}^{N-1}\binom{N+k-1}{k}\left(K_\zeta e^{-K}\right)^N\frac{\left(\frac{\Omega}{2\sigma_n^2}\right)^k}{\left(\frac{\Omega}{2\sigma_n^2}+K_\zeta\right)^{k+N}}. \tag{74}$$

Asymptotically, this CDF can be represented as

$$F_\zeta^{\infty}(\zeta|E_0) = 1 - \binom{2N-1}{N}\left(\frac{K_\zeta e^{-K}}{\frac{\Omega}{2\sigma_n^2}+K_\zeta}\right)^N.$$

By substituting the CDFs into average SER, a closed form can be obtained form by summation of infinite series. Moreover, by replacing the obtained CDFs with the asymptotic CDFs, the asymptotic average SER can be obtained in a closed-form.

6 Numerical Results

This section presents analytical and simulation results of MASK modulation with coherent, noncoherent and amplitude-coherent detection in flat Rician fading channels. Moreover, the AC detection is evaluated using the optimum, suboptimum, and the heuristic detectors with single and antennas reception using various modulation orders. The Monte Carlo simulation results are obtained by generating 10^7 realizations and the average SNR is defined as $SNR = \frac{\Omega\ \bar{P}_s}{2\sigma_h^2}$, where $\bar{E}_s = \frac{1}{M}\sum_{m=0}^{M-1}E_m$ is the average transmission power. In the analytical results, the summations with infinite

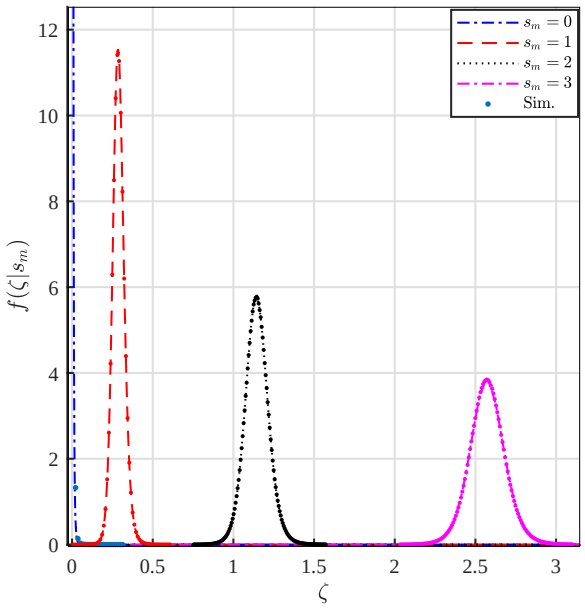

Figure 1: Analytical and simulated conditional PDF $f\left(\zeta|E_m\right)$ for $M = 4$, $K = 10$ and $SNR = 27$ dB.

limits are truncated where 20 terms are used. For the results included in this section $\bar{P}_s$ and Ω are normalized to 1. The figures' legends are using the following abbreviations, simulation (Sim.), analytical (Anal.), coherent detector (Coh.), noncoherent detector (NC), near-optimum AC (AC-NO), suboptimum AC (AC-SO), AC heuristic (AC-H), and asymptotic (Asymp.).

Fig. 1 shows the analytical and simulated conditional PDF $f\left(\zeta|E_m\right)$, for the case of $M = 4$, $K = 10$ and $SNR = 27$ dB. As can be noted from the figure, the overlap between the conditional PDF for different E_m values at high SNRs is negligible, and thus, the transmitted signal can be recovered reliably by using the suitable threshold as described in (33) for the heuristic AC detector. However, because the conditional PDFs are not identical and not equally spaced, the probability of error given E_m will not be equal. Consequently, the amplitudes of the transmitted signals can be optimized to minimize the BER. Nevertheless, the improvement that would be gained is generally limited as reported for the Rayleigh fading case [30].

Figs. 2 and 3 compare the SER of the coherent and heuristic AC detectors using $M = 2$ and 4, respectively. The figures also show the SER when the number of receiving antennas $N = 1$, 2, and 4.The Rician factor for both figures is fixed at $K = 4$. The results presented in both figures show that the simulated SER perfectly matches the analytical SER for all the considered M and N values. Comparing the coherent and AC heuristic detector for the case of $M = 2$ in Fig. 2 show that the coherent detector outperforms the AC detector by about 3 dB at $P_e = 5 \times 10^{-5}$. For the case of $M = 4$ shown in Fig. 3, the difference between the coherent and AC Heuristic becomes smaller and dependent on N. More specifically, the difference becomes about 1.4, 1.7 and 2.0 dB for $N = 1$, 2, and 3, respectively, at $P_e = 5 \times 10^{-5}$.

Fig. 4 illustrates the impact of the Rician factor K on the SER for the cases of $M = 2$ and 4, for a single receiving antenna, $N = 1$. The results for $K = 0$ are considered as the worst case scenario where the channel becomes Rayleigh. As can be depicted from the figure, the SER of the AC detector may improve substantially for large values of K. Nevertheless, the SER improvement gained by increasing K is higher for $M = 2$ as compared with the $M = 4$ case, which is due to the fact that higher order modulations are more sensitive to AWGN, and thus, the fading will be less dominant as compared to low order modulations. For example, the SER improvement by increasing K from 1 to 20 is about 20 dB for $M = 2$, while it is about 18 dB for $M = 4$, at $P_e = 4 \times 10^{-4}$.

Figs. 5 and 6 compare the SER performance of the near optimum, suboptimum and heuristic AC detectors for

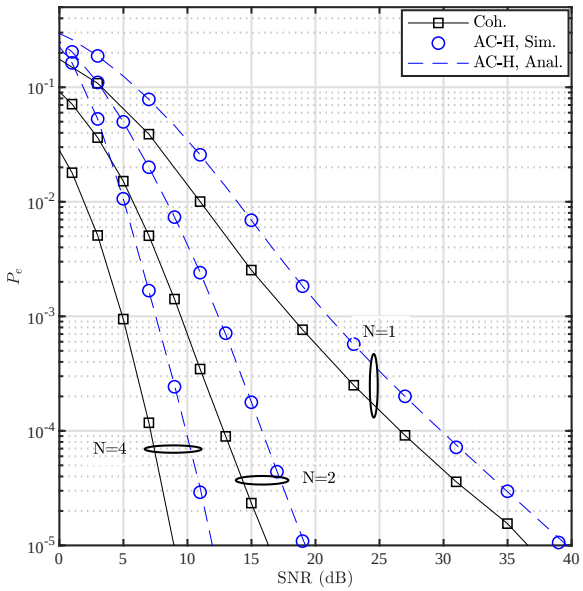

Figure 2: Analytical and simulated SER of the AC heuristic (AC-H) and coherent detectors using $N = 1, 2, 4$, $M = 2$, and $K = 4$.

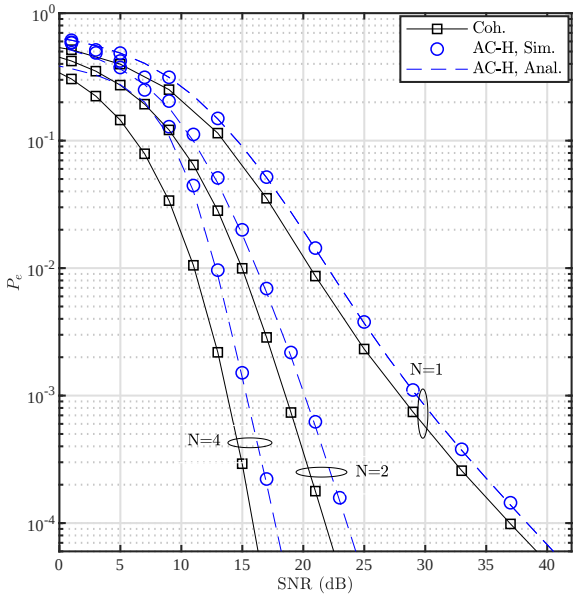

Figure 3: Analytical and simulated SER of the AC heuristic (AC-H) and coherent detectors using $N = 1, 2, 4$, $M = 4$, and $K = 4$.

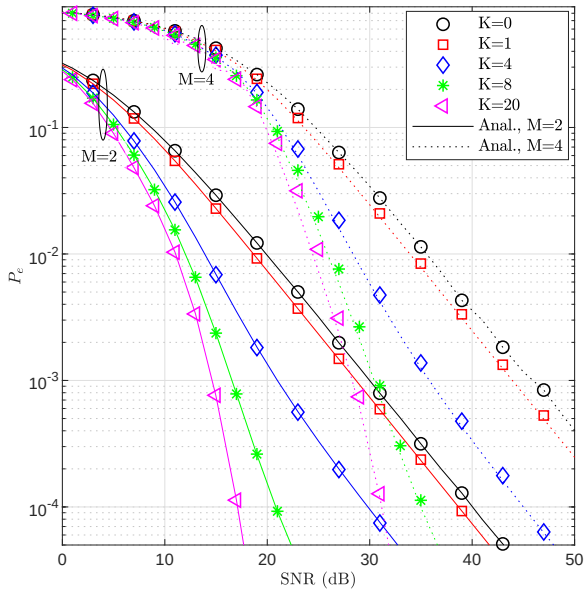

Figure 4: Analytical and simulated SER of the AC heuristic (AC-H) detector using $M = 2$ and 4 for different values of K, $N = 1$.

$M = 2$ and 4, respectively, and the results are obtained using $K = 4$. As shown in both figures, the heuristic detector outperforms the suboptimum for all cases. For $M = 2$, the difference is about 3.5 and 3.7 dB for $N = 1$ and 2, respectively. For $M = 4$, the difference is about 2.5 and 3 dB for $N = 1$ and 2, respectively. As expected, the near-optimum detector outperforms the heuristic for $SNR \lesssim 21$ dB for $M = 2$ and $N = 1$, which corresponds the low and moderate SNRs. For $N = 2$, the system SNR is generally much smaller that the $N = 1$ case, and hence, near-optimum detector outperforms the heuristic. The SER for the $M = 4$ case in Fig. 6 is generally similar to the $M = 2$ case, except that the cross-over point is shifted to $SNR \approx 29$ dB. Consequently, the heuristic detector offers the best compromise between SER and computational complexity as compared to the suboptimum and near-optimum detectors.

Fig. 7 presents the system SER using the optimum noncoherent and the heuristic AC detector given that $M = 2$ and 4, $N = 1$, and $K = 4$. As can be noted from the figure, the noncoherent detector outperforms the heuristic for SNRs less than 11 and 5 dB, for $M = 2$ and 4 respectively. Nevertheless, the noncoherent detector SER deteriorates severely for $M > 2$ where an error floor is observed at $SER \sim 10^{-1}$. Moreover, it is worth noting that the optimum noncoherent detector requires prior knowledge of the channel statistical values.

Figs. 8 and 9 show the effect of the phase noise on both the heuristic and coherent detectors for the cases of $M = 2$ and 4, respectively. The parameters for the two figures are $N = 1$ and $K = 4$ while the phase noise is modeled as a Tikhonov random variable with variance $\sigma_\phi^2 = [0, 3, 5, 7, 10]$. In both figures, the SER of the AC detector is represented by a single curve because it is immune to phase noise. The results in Figs. 8 and 9 show clearly the advantage of the heuristic detector in the presence of phase noise, particularly at high SNRs, where coherent detector exhibits SER error floors. As expected, the $M = 4$ case is more sensitive than the $M = 2$, even for very small values of σ_ϕ^2.

Fig. 10 compares the asymptotic and analytical SERs using $M = 2$, $K = 4$, $N = 1$, 2 and 3. As can be noted from the figure, the asymptotic SER provides accurate results for the SER at high SNRs, and thus, it can be used to simplify the SER analysis.

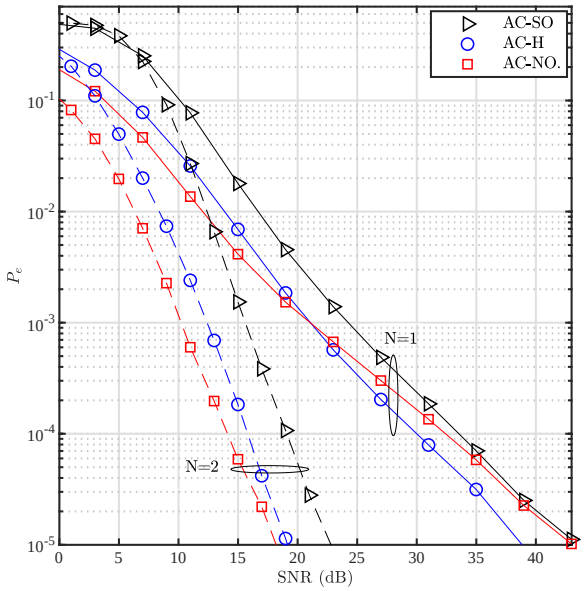

Figure 5: SER for of the near optimum (AC-NO), suboptimum (AC-SO), and heuristic AC (AC-H) detectors using $N = 1$, 2, $M = 2$, and $K = 4$.

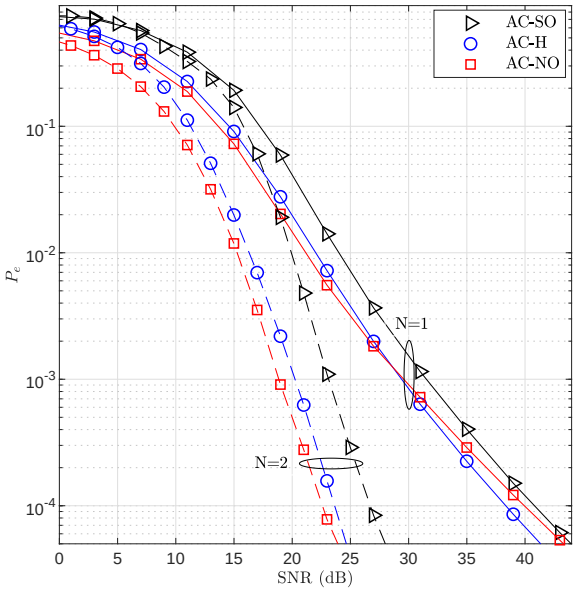

Figure 6: SER for of the near optimum (AC-NO), suboptimum (AC-SO) and heuristic AC (AC-H) detectors using $N = 1$, 2, $M = 4$, and $K = 4$.

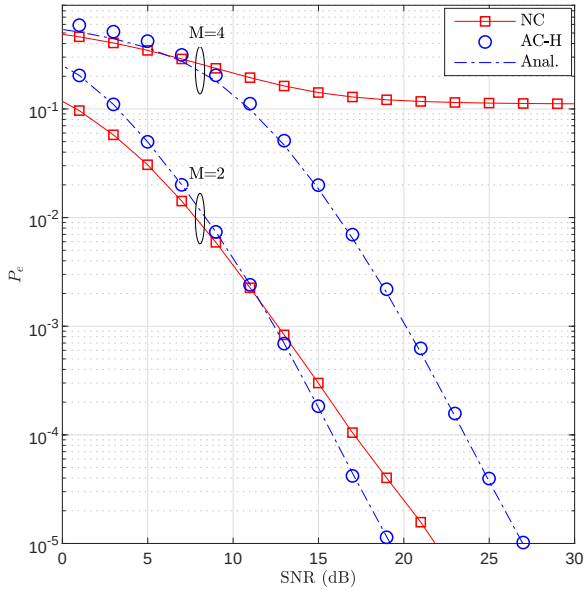

Figure 7: The SER for the noncoherent (NC) and heuristic (AC-H) detectors using $M = 1$ and 2, $N = 1$ and $K = 4$.

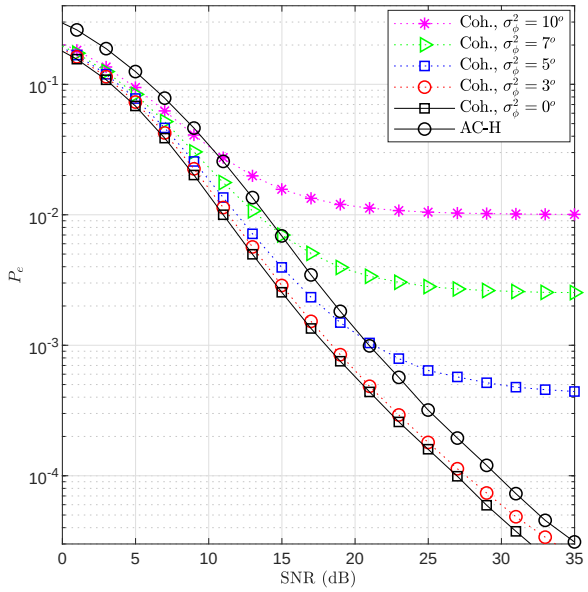

Figure 8: The effect of the phase noise on the heuristic AC (AC-H) and coherent detectors for $N = 1$, where $M = 2$, $K = 4$.

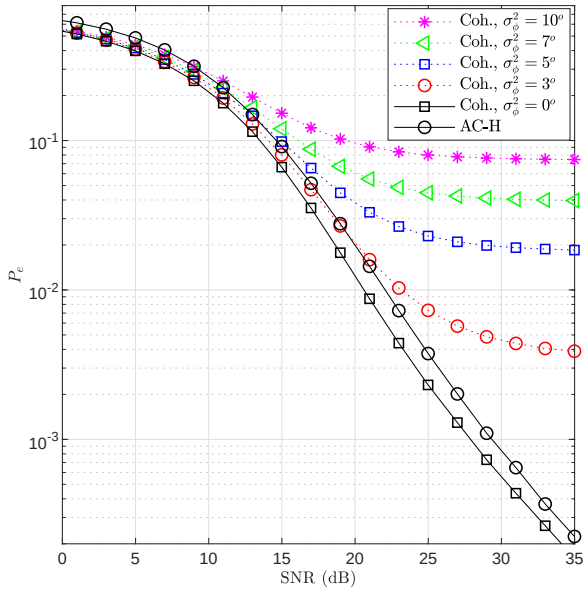

Figure 9: The effect of the phase noise on the heuristic AC (AC-H) and coherent detectors for $N = 1$, where $M = 4$, $K = 4$.

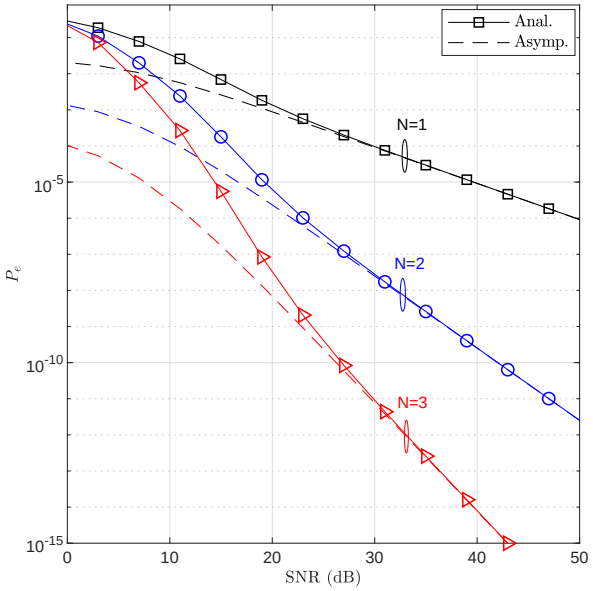

Figure 10: Asymptotic SER using $M = 2$, $K = 4$, and $N = 1, 2$ and 3.

7 Conclusion and Future Work

In this paper, the SER performance of MASK modulation with amplitude-coherent detection has been considered over flat Rician fading channels with receiver diversity. The optimum, near-optimum and suboptimum amplitude-coherent detectors were derived for the Rician channel and their SER was compared with the coherent and noncoherent detectors for various modulation orders and number of receiving antennas. The SER of the heuristic detector was derived analytically using different approaches, and the asymptotic SER was derived for high SNRs. The obtained analytical and simulation results confirm that the amplitude-coherent detection offers the SER performance that is comparable to the coherent detection, but without the need for a prior knowledge of the channel phase. Consequently, the computational complexity of the amplitude coherent detector is much less than the coherent detector and it is more robust to phase noise and phase estimation errors.

References

[1] A. Al-Dweik and Y. Iraqi, "Error probability analysis and applications of amplitude-coherent detection in flat Rayleigh fading channels," *IEEE Trans. Commun.*, vol. 64, no. 5, pp. 2235–2244, May 2016.

[2] Digital Video Broadcasting (DVB); Framing Structure, Channel Coding and Modulation for Digital Terrestrial Television, ETSI Standard EN 300744 v1.6.1, 2008.

[3] IEEE Standard for Local and metropolitan area networks Part 16: Air Interface for Broadband Wireless Access Systems Amendment 3: Advanced Air Interface, IEEE Standard 802.16m, 2011.

[4] LTE; Evolved Universal Terrestrial Radio Access (E-UTRA), LTE Physical Layer, 3GPP TS 36.300, 2011.

[5] F. Yang and L.-L. Yang, "Low-complexity noncoherent fusion rules for wireless sensor networks monitoring multiple events," *IEEE Trans. Aerosp. Electron. Syst.*, vol. 50, no. 3, pp. 2343–2353, Jul. 2014.

[6] S. Bi, C. K. Ho, and R. Zhang, "Wireless powered communication: Opportunities and challenges," *IEEE Commun. Mag.*, vol. 53, no. 4, pp. 117-125, Apr. 2015.

[7] M. Al-Jarrah, A. Al-Dweik, E. Alsusa, and E. Damiani, "RFID reader localization using hard decisions with error concealment," submitted to *IEEE Sensors J.*

[8] Z. Zhao, Z. Zhang, J. Tan, Y. Liu, and J. Liu, "200 Gb/s FSO WDM communication system empowered by multiwavelength directly modulated TOSA for 5G wireless networks," *IEEE Photon. J.*, vol. 10, no. 4, pp. 1-8, Aug. 2018.

[9] J. Rodríguez, D. Lamar, P. Miaja, and J. Sebastián, "Reproducing single-carrier digital modulation schemes for VLC by controlling the first switching harmonic of the DC–DC power converter output voltage ripple," *IEEE Trans. Power Electron.*, vol. 33, no. 9, pp. 7994-8010, Sep. 2018.

[10] A. Belmonte and J. M. Kahn, "Performance of synchronous optical receivers using atmospheric compensation techniques," *Opt. Express*, vol. 16, no. 18, pp. 14151-14162, Sep. 2008.

[11] A. Touati, A. Abdaoui, F. Touati, M. Uysal, and A. Bouallegue, "On the effects of combined atmospheric fading and misalignment on the hybrid FSO/RF transmission," *IEEE/OSA J. Opt. Commun. Netw.*, vol. 8, no. 10, pp. 715-725, Oct. 2016.

[12] P. Trinh, T. Thang, and A. Pham, "Mixed mmwave RF/FSO relaying systems over generalized fading channels with pointing errors," *IEEE Photon. J.*, vol. 9, no. 1, pp. 1-14, Feb. 2017.

[13] M. A. Khalighi and M. Uysal, "Survey on free space optical communication: A communication theory perspective," *IEEE Commun. Surveys Tuts.*, vol. 16, no. 4, pp. 2231-2258, 2014.

[14] D. Tsonev, S. Sinanovic and H. Haas, "Complete modeling of nonlinear distortion in OFDM-based optical wireless communication," *J. Lightw. Technol.*, vol. 31, no. 18, pp. 3064-3076, Sep. 2013.

[15] H. Lu, C. Li, C. Ho, M. Cheng, X. Lin, Z. Yang, and H. Chen, "64 Gb/s PAM4 VCSEL-based FSO link," *Opt. Express*, vol. 25, no. 5, pp. 5749-5757, Mar. 2017.

[16] J. Armstrong and B. Schmidt, "Comparison of asymmetrically clipped optical OFDM and DC-biased optical OFDM in AWGN," *IEEE Commun. Lett.*, vol. 12, no. 5, pp. 343-345, May 2008.

[17] M. Zhang and Z. Zhang, "An optimum DC-biasing for DCO-OFDM system," *IEEE Commun. Lett.*, vol. 18, no. 8, pp. 1351-1354, Aug. 2014.

[18] N. Letzepis and A. Fabregas, "Outage probability of the freespace optical channel with doubly stochastic scintillation," *IEEE Trans. Commun.*, vol. 57, no. 10, pp. 2899–2902, Oct. 2009.

[19] S. Aghajanzadeh and M. Uysal, "Diversity-multiplexing trade-off in coherent free-space optical systems with multiple receivers," *IEEE/OSA J. of Opt. Commun. Netw.*, vol. 2, no. 12, pp. 1087-1094, Dec. 2010.

[20] K. Jung, S. S. Nam, Y. Ko and M. Alouini, "BER Performance of FSO Links over Unified Channel Model for Pointing Error Models," *IEEE Int. Conf. Commun.*, (ICC), Kansas City, MO, 2018, pp. 1-6.

[21] F. Yang, J. Cheng and T. A. Tsiftsis, "Free-space optical communications with generalized pointing errors," *IEEE Int. Conf. Commun.* (ICC), Budapest, 2013, pp. 3943-3947.

[22] I. S. Ansari, M. Alouini and J. Cheng, "On the capacity of FSO links under Lognormal and Rician-Lognormal turbulences," *IEEE 80th Veh. Technol. Conf.* (VTC2014-Fall), Vancouver, BC, 2014, pp. 1-6.

[23] D. Yue, Y. Zhang, and Y. Jia, "Beamforming based on specular component for massive MIMO systems in Ricean fading," *IEEE Wireless Commun. Lett.*, vol. 4, no. 2, pp. 197-200, Apr. 2015.

[24] S. Jin, D. Yue, and H. Nguyen, "Equal-gain transmission in massive MIMO systems under Ricean fading," *IEEE Trans. Veh. Technol.*, vol. 67, no. 10, pp. 9656-9668, Oct. 2018.

[25] H. Tataria, P. Smith, L. Greenstein, and P. Dmochowski, "Zero-forcing precoding performance in multiuser MIMO systems with heterogeneous Ricean fading," IEEE Wireless Commun. Lett., vol. 6, no. 1, pp. 74-77, Feb. 2017.

[26] J. Nyarko, J. Xie, R. Yao, Y. Wang, and L. Wang, "Accurate approximation of ZF massive MIMO channel rate with a finite antenna over Ricean fading channel," *IEEE Access*, vol. 6, pp. 65803-65812, 2018.

[27] X. Sun, K. Xu, W. Ma, Y. Xu, X. Xia, and D. Zhang, "Multi-pair two-way massive MIMO AF full-duplex relaying with imperfect CSI over Ricean fading channels," *IEEE Access*, vol. 4, pp. 4933-4945, 2016.

[28] R. Sun and D. W. Matolak, "Air–Ground Channel Characterization for Unmanned Aircraft Systems Part II: Hilly and Mountainous Settings," IEEE Transactions on Vehicular Technology, vol. 66, no. 3, pp. 1913-1925, March 2017.

[29] D. W. Matolak and R. Sun, "Air–Ground Channel Characterization for Unmanned Aircraft Systems—Part III: The Suburban and Near-Urban Environments," IEEE Transactions on Vehicular Technology, vol. 66, no. 8, pp. 6607-6618, Aug. 2017.

[30] L. Bariah, A. Al-Dweik, S. Muhaidat, Y. Iraqi, and M. Al-Mualla, "Performance analysis of semi-coherent OFDM systems with imperfect channel estimates", *IEEE Trans. Veh. Technol.*, vol. 677, no. 11, pp. 10773-10787, Nov. 2018.

[31] R. K. Mallik, R. D. Murch and Y. Li, "Channel magnitude based energy detection with receive diversity for multi-level amplitude-shift keying in Rayleigh fading," *IEEE Trans. Commun.*, vol. 65, no. 7, pp. 3079-3094, Jul. 2017.

[32] R. Dana, "Statistics of sampled Rician fading," DNA-TR-92–98 Tech. Rep., Feb. 1993.

[33] A. Saci, A. Al-Dweik, A. Shami and Y. Iraqi, "One-shot blind channel estimation for OFDM systems over frequency-selective fading channels," *IEEE Trans. Commun.*, vol. 65, no. 12, pp. 5445-5458, Dec. 2017.

[34] I. B. G. Pôrto and M. D. Yacoub, "On the Phase Statistics of the κ-μ Process," *IEEE Trans. Wireless Commun.*, vol. 15, no. 7, pp. 4732-4744, July 2016.

[35] I. Gradshteyn and I. Ryzhik, Table of Integrals, Series and Products, 7th ed. USA: Academic Press, 2000.

[36] M. Abramowitz and I. Stegun, Handbook of Mathematical Functions with Formulas, New York, 1972.

[37] J. Proakis and M. Salehi, Digital Communications, 5th ed. UK: Ashford Colour Press, 2014.

[38] S. András, Á. Baricz, and Y. Sun, "The generalized Marcum Q-function: An orthogonal polynomial approach," *Acta Univ. Sapientiae Math.*, vol. 3, no. 1, pp. 60–76, 2011.

[39] A. P. Prudnikov, Yu. A. Brychkov, and O. I. Marichev. Integrals and Series, Volume 2 Special Functions. Gordon and Breach Science Publishers, UK, 3rd edition, 1986.

[40] M. K. Simon and M.-S. Alouini, Digital Communication over Fading Channels: A Unified Approach to Performance Analysis, 2nd ed. NY: A Wiley-Interscience Publication, 2000.

Appendix I: Evaluating the integral $\mathcal{I}_\theta$

The integral $\mathcal{I}_\theta$ given in (23) can be written as

$$\mathcal{I}_\theta = \frac{1}{2\pi}\int_{-\pi}^{\pi} \exp\left(2\sqrt{K\left(K+1\right)}\cos\left(\theta-\phi\right) + \frac{\alpha s_m}{\sigma_n^2}\left|r\right|\cos\left(\theta-\theta_{\rm r}\right)\right) d\theta. \tag{75}$$

Applying the trigonometric identity $\cos\left(\theta-\phi\right) = \cos\theta\cos\phi + \sin\theta\sin\phi$ yields

$$\begin{aligned}\mathcal{I}_\theta &= \frac{1}{2\pi}\int_{-\pi}^{\pi} \exp\left(2\sqrt{K\left(K+1\right)}\left(\cos\left(\theta\right)\cos\left(\phi\right)+\sin\left(\theta\right)\sin\left(\phi\right)\right) + \frac{\alpha s_m}{\sigma_n^2}\left|r\right|\left(\cos\left(\theta\right)\cos\left(\theta_{\rm r}\right)+\sin\left(\theta\right)\sin\left(\theta_{\rm r}\right)\right)\right) d\theta \\ &= \frac{1}{2\pi}\int_{-\pi}^{\pi} \underbrace{\exp\left(\left(A+B\alpha s_m\left|r\right|\right)\cos\left(\theta\right) + \left(C+D\alpha s_m\left|r\right|\right)\sin\left(\theta\right)\right)}_{g(\theta)} d\theta \end{aligned} \tag{76}$$

where $A = 2\sqrt{K\left(K+1\right)}\cos\left(\phi\right)$, $B = \frac{1}{\sigma_n^2}\cos\left(\theta_{\rm r}\right)$, $C = 2\sqrt{K\left(K+1\right)}\sin\left(\phi\right)$ and $D = \frac{1}{\sigma_n^2}\sin\left(\theta_{\rm r}\right)$.

It should be observed that the function $g\left(\theta\right)$ is not symmetric at $\theta = 0$, and thus $\int_{-\pi}^{\pi} g\left(\theta\right) d\theta \neq 2\int_{0}^{\pi} g\left(\theta\right) d\theta$. However, the main interest is to evaluate the integral of $g\left(\theta\right)$ rather than calculating the value of $g\left(\theta\right)$ itself. Therefore, a mathematical manipulation can be made to force symmetry of $g\left(\theta\right)$ at $\theta = 0$ without affecting the value of the integral $\mathcal{I}_\theta$. Towards this goal, first the value of θ at which the function $g\left(\theta\right)$ has a global maximum, φ, is evaluated, and then

the function is shifted by the same value in order to have the maximum at $\theta = 0$. Then, the integral can be divided into two intervals

$$\int_{-\pi}^{\pi} g(\theta)\, d\theta = \int_{-\pi}^{\pi} g(\theta+\varphi)\, d\theta = 2\int_{0}^{\pi} g(\theta+\varphi)\, d\theta. \tag{77}$$

Then, the resulting integral is evaluated numerically by applying Gauss-Chebyshev quadrature rule.

$$\frac{dg(\theta)}{d\theta} = \left[-\left(A + B\alpha s_m |r|\right)\sin\theta + \left(C + D\alpha s_m |r|\right)\cos\theta\right] \exp\left(\left(A + B\alpha s_m |r|\right)\cos\theta + \left(C + D\alpha s_m |r|\right)\sin\theta\right). \tag{78}$$

To find $\varphi \in (-\pi, \pi)$, the unique root of $\frac{dg(\theta)}{d\theta} = 0$ is calculated,

$$\varphi = \tan^{-1}\left(\frac{C + D\alpha s_m |r|}{A + B\alpha s_m |r|}\right). \tag{79}$$

Thus, the symmetric function around $\theta = 0$, $g(\theta+\varphi)$, can be written as

$$g(\theta+\varphi) = \exp\left(\left(A + B\alpha s_m |r|\right)\cos(\theta+\varphi) + \left(C + D\alpha s_m |r|\right)\sin(\theta+\varphi)\right). \tag{80}$$

Therefore, the integral $\mathcal{I}_\theta$ given in (76) can be rewritten as as

$$\mathcal{I}_\theta = 2\int_{0}^{\pi} g(\theta+\varphi)\, d\theta. \tag{81}$$

Evaluating the integral $\mathcal{I}_\theta$ by substitution, setting $y = \cos(\theta)$, yields

$$\mathcal{I}_\theta = \frac{1}{\pi}\int_{-1}^{1} \frac{1}{\sqrt{1-y^2}} \exp\left\{\left(A + B\alpha s_m |r|\right)\cos\left(\varphi + \cos^{-1}(y)\right) + \left(C + D\alpha s_m |r|\right)\sin\left(\varphi + \cos^{-1}(y)\right)\right\} dy$$

which can be efficiently solved applying Gauss-Chebyshev quadrature rules [36]

$$\mathcal{I}_\theta = \frac{1}{L}\sum_{l=1}^{n} \exp\left[\left(A + B\alpha s_m |r|\right) f_{\mathrm{c}}(y_l) + \left(C + D\alpha s_m |r|\right) f_{\mathrm{s}}(y_l)\right], \tag{82}$$

where $f_{\mathrm{c}}(y_l) = \cos\left(\varphi + \cos^{-1}(y_l)\right) = \cos\left(\varphi + \frac{2l-1}{2L}\pi\right)$, $f_{\mathrm{s}}(y_l) = \sin\left(\varphi + \cos^{-1}(y_l)\right) = \sin\left(\varphi + \frac{2l-1}{2L}\pi\right)$ and $y_l = \cos\left(\frac{2l-1}{2L}\pi\right)$.

Appendix II: Evaluating $F_\zeta(\zeta|E_m)$, $m > 0$

To obtain the PDF $\mathrm{f}(\zeta|E_m)$, averaging $\mathrm{f}(\zeta|x, E_m)$ over $\mathrm{f}(x)$ is needed, which yields

$$f(\zeta|E_m) = \int_0^\infty f(\zeta|x, E_m)\ f(x)\, dx \tag{83}$$

$$= \frac{\exp\left(-\frac{\lambda}{2}\right)}{4\sigma_n^2\sigma_h^2} E_m^{-0.5(N-1)} \left(\sigma_h^2\lambda\right)^{-0.5(N-1)} \zeta^{0.5(N-1)} \times \int_0^\infty x^{0.5(N+1)} \exp\left(-\left(\frac{\zeta + E_m}{2\sigma_n^2} + \frac{1}{2\sigma_h^2}\right)x\right) \mathrm{I}_{N-1}\left(\frac{\sqrt{E_m\,\zeta}}{\sigma_n^2}x\right) \mathrm{I}_{N-1}\left(\sqrt{\frac{\lambda}{\sigma_h^2}}\sqrt{x}\right) dx. \tag{84}$$

Substituting the two approximations (43) and (44) in (84) yields

$$f\left(\zeta|E_m\right)=\frac{\lambda^{-0.5(N-1)}\exp\left(-\frac{\lambda}{2}\right)}{4\sigma_n^2\sqrt{\frac{2\pi}{\sigma_n^2}}}E_m^{-0.5(N-1)}\frac{\zeta^{0.5(N-1)}\left(I_A+I_B\right)}{\sqrt[4]{E_m\,\zeta}},$$

where I_A and I_B are given by

$$I_A=\int_0^\infty x^{0.5N}\exp\left(-C_\zeta x\right)\sum_{l=0}^{\infty}\frac{\left(\frac{\lambda}{4\sigma_h^2}\right)^{\frac{2l+N-1}{2}}}{l!\Gamma\left(l+N\right)}x^{\frac{2l+N-1}{2}}dx \tag{85}$$

$$I_B=\int_0^\infty x^{0.5N}\exp\left(-C_\zeta x\right)\sum_{l=0}^{\infty}\frac{\left(\frac{\lambda}{4\sigma_h^2}\right)^{\frac{2l+N-1}{2}}x^{\frac{2l+N-1}{2}}}{l!\Gamma\left(l+N\right)}\sum_{q=1}^{Q}\frac{(-1)^q}{x^q}\frac{\prod_{k=1}^{q}\left[4\left(N-1\right)^2-\left(2k-1\right)^2\right]}{q!8^q\left(\frac{\sqrt{E_m\,\zeta}}{\sigma_n^2}\right)^q}dx. \tag{86}$$

The integral I_A can be evaluated as

$$\begin{aligned}I_A&=\int_0^\infty x^{0.5N}\exp\left(-C_\zeta x\right)\sum_{l=0}^{\infty}\frac{1}{l!\Gamma\left(l+N\right)}\left(\frac{\lambda}{4\sigma_h^2}\right)^{\frac{2l+N-1}{2}}x^{\frac{2l+N-1}{2}}dx\\&=\sum_{l=0}^{\infty}\frac{1}{l!\Gamma\left(l+N\right)}\left(\frac{\lambda}{4\sigma_h^2}\right)^{\frac{2l+N-1}{2}}\int_0^\infty x^{l+N-0.5}\exp\left(-C_\zeta x\right)dx.\end{aligned} \tag{87}$$

By substituting $y=\left(\frac{\zeta+E_m}{2\sigma_n^2}+\frac{1}{2\sigma_h^2}-\frac{\sqrt{E_m\,\zeta}}{\sigma_n^2}\right)x$ in (87), can be evaluated as

$$\begin{aligned}I_A&=\sum_{l=0}^{\infty}\frac{1}{l!\Gamma\left(l+N\right)}\left(\frac{\lambda}{4\sigma_h^2}\right)^{\frac{2l+N-1}{2}}\frac{1}{C_\zeta^{l+N+0.5}}\int_0^\infty y^{l+N-0.5}\exp\left(-y\right)dy\\&=\sum_{l=0}^{\infty}\frac{1}{l!\Gamma\left(l+N\right)}\left(\frac{\lambda}{4\sigma_h^2}\right)^{\frac{2l+N-1}{2}}\frac{1}{C_\zeta^{l+N+0.5}}\Gamma\left(l+N+0.5\right)\\&=\sum_{l=0}^{\infty}\frac{A_l}{C_\zeta^{l+N+0.5}},\end{aligned} \tag{88}$$

The integral I_B can be evaluated as following

$$\begin{aligned}I_B&=\int_0^\infty x^{0.5N}\exp\left(-C_\zeta x\right)\sum_{q=1}^{Q}\frac{(-1)^q}{x^q}\frac{\prod_{k=1}^{q}\left[4\left(N-1\right)^2-\left(2k-1\right)^2\right]}{q!8^q\left(\frac{\sqrt{E_m\,\zeta}}{\sigma_n^2}\right)^q}\\&\times\sum_{l=0}^{\infty}\frac{1}{l!\Gamma\left(l+N\right)}\left(\frac{\lambda}{4\sigma_h^2}\right)^{\frac{2l+N-1}{2}}x^{\frac{2l+N-1}{2}}dx\end{aligned} \tag{89}$$

$$\begin{aligned}&=\sum_{q=1}^{Q}\sum_{l=0}^{L=\infty}\frac{(-1)^q}{l!\Gamma\left(l+N\right)}\left(\frac{\lambda}{4\sigma_h^2}\right)^{\frac{2l+N-1}{2}}\frac{\prod_{k=1}^{q}\left[4\left(N-1\right)^2-\left(2k-1\right)^2\right]}{q!8^q\left(\frac{\sqrt{E_m\,\zeta}}{\sigma_n^2}\right)^q}\\&\times\int_0^\infty x^{N-q+l-0.5}\exp\left(-C_\zeta x\right)dx.\end{aligned} \tag{90}$$

Substituting $y = \left(\frac{\zeta+E_m}{2\sigma_n^2} + \frac{1}{2\sigma_h^2} - \frac{\sqrt{E_m\ \zeta}}{\sigma_n^2}\right) x$ yields

$$I_B = \sum_{q=1}^{Q}\sum_{l=0}^{L=\infty} \frac{(-1)^q}{l!\Gamma\left(l+N\right)} \left(\frac{\lambda}{4\sigma_h^2}\right)^{\frac{2l+N-1}{2}} \left(\frac{\prod_{k=1}^{q}\left[4\left(N-1\right)^2-\left(2k-1\right)^2\right]}{q!8^q\left(\frac{\sqrt{E_m\ \zeta}}{\sigma_n^2}\right)^q}\right)$$
$$\times \frac{1}{C_\zeta^{N-q+l+0.5}} \int_0^\infty y^{N-q+l-0.5}\exp\left(-y\right)dy \tag{91}$$
$$= \sum_{q=1}^{Q}\sum_{l=0}^{\infty} \frac{B_q^l}{\zeta^{0.5q} C_\zeta^{N-q+l+0.5}}. \tag{92}$$

Finally, $\mathrm{f}\left(\zeta|E_m\right)$ is obtained as

$$f\left(\zeta|E_m\right) = C\ \left(\sum_{l=0}^{\infty} \frac{A_l \zeta^{0.5N-0.75}}{C_\zeta^{(l+N+0.5)}} + \sum_{q=1}^{Q}\sum_{l=0}^{\infty} \frac{B_q^l \zeta^{0.5N-0.5q-0.75}}{C_\zeta^{(N-q+l+0.5)}}\right) \tag{93}$$

The CDF can be evaluated as

$$F_\zeta\left(\zeta|E_m>0\right) = \int_0^\zeta f\left(\zeta|E_m\right)d\zeta$$
$$= C\left(\sum_{l=0}^{\infty} A_l \mathcal{I}_A^l + \sum_{q=1}^{Q}\sum_{l=0}^{\infty} B_q^l \mathcal{I}_B^{q,l}\right), \tag{94}$$

where

$$\mathcal{I}_A^l = \int_0^\zeta \zeta^{0.5N-0.75} C_\zeta^{-(l+N+0.5)} d\zeta \tag{95}$$
$$\mathcal{I}_B^{q,l} = \int_0^\zeta \zeta^{0.5N-0.5q-0.75} C_\zeta^{-(N-q+l+0.5)} d\zeta. \tag{96}$$

It should be observed that both integrals have the same form, and thus they can be rewritten as

$$\mathcal{I} = \int_0^\zeta \zeta^a C_\zeta^b d\zeta \tag{97}$$
$$= \int_0^\zeta \zeta^a \left(\frac{\zeta}{2\sigma_n^2} - \frac{\sqrt{E_m\ \zeta}}{\sigma_n^2} + c\right)^b d\zeta, \tag{98}$$

Substituting $y = \sqrt{\zeta}$, the integrals $\mathcal{I}_A^l$ and $\mathcal{I}_B^{q,l}$ have the following form

$$\mathcal{I} = 2\int_0^{\sqrt{\zeta}} y^{2a+1}\left(\frac{y^2}{2\sigma_n^2} - \frac{\sqrt{E_m}}{\sigma_n^2}y + c\right)^b dy. \tag{99}$$

It should be noticed that integrals of this form can be solved in recursive manner according to [35, 2.17, page 79].

8 Appendix III: Evaluating $F_\zeta(\zeta|E_m)$, $m=0$

Averaging $f(\zeta|x,E_m)$, $m=0$ over $\mathrm{f}(x)$ yields

$$\begin{aligned} f(\zeta|E_m) &= \int_0^\infty f(\zeta|x,E_m)\ f(x)\,dx \\ &= \frac{\lambda_0^N\left(\lambda_0\sigma_h^2\right)^{-0.5(N-1)}}{2\sigma_h^2(N-1)!\exp\left(\frac{\lambda_0}{2}\right)}\zeta^{N-1}\int_0^\infty x^{1.5N-0.5}\exp\left[-x\left(\lambda_0\zeta+\frac{1}{2\sigma_h^2}\right)\right]\mathrm{I}_{N-1}\left(\sqrt{\frac{\lambda_0 x}{\sigma_h^2}}\right)dx. \end{aligned} \tag{100}$$

Substituting the approximation given in (43) in (100) yields,

$$f(\zeta|E_m) = \frac{\lambda_0^N}{(N-1)!}\frac{1}{2\sigma_h^2}(\zeta)^{N-1}\left(\frac{1}{\lambda_0\sigma_h^2}\right)^{0.5(N-1)}\exp\left(-\frac{\lambda_0}{2}\right)\sum_{l=0}^{\infty}\frac{1}{l!\Gamma(l+N)}\left(\frac{\lambda_0}{4\sigma_h^2}\right)^{\frac{2l+N-1}{2}}I_0^l, \tag{101}$$

where

$$I_0^l = \int_0^\infty x^{2N+l-1}\exp\left(-\left(\lambda_0\ \zeta+\frac{1}{2\sigma_h^2}\right)x\right)dx. \tag{102}$$

Substituting $y=\left(\lambda_0\ \zeta+\frac{1}{2\sigma_h^2}\right)x$ in (102), I_0^l can be obtained as

$$\begin{aligned} I_0^l &= \frac{1}{\left(\lambda_0\ \zeta+\frac{1}{2\sigma_h^2}\right)^{2N+l}}\int_0^\infty (y)^{2N+l-1}\exp(-y)\,dy \\ &= \frac{1}{\left(\lambda_0\ \zeta+\frac{1}{2\sigma_h^2}\right)^{2N+l}}\Gamma(2N+l). \end{aligned} \tag{103}$$

Consequently, $\mathrm{f}(\zeta|E_m)$ can be expressed as

$$f(\zeta|E_m) = C_0\ \zeta^{N-1}\sum_{l=0}^{\infty}\frac{\Gamma(2N+l)}{l!\Gamma(l+N)}\left(\frac{\lambda_0}{4\sigma_h^2}\right)^{\frac{2l+N-1}{2}}\left(\lambda_0\zeta+\frac{1}{2\sigma_h^2}\right)^{-(2N+l)},\ m=0. \tag{104}$$